

RESEARCH ARTICLE | MAY 27 2021

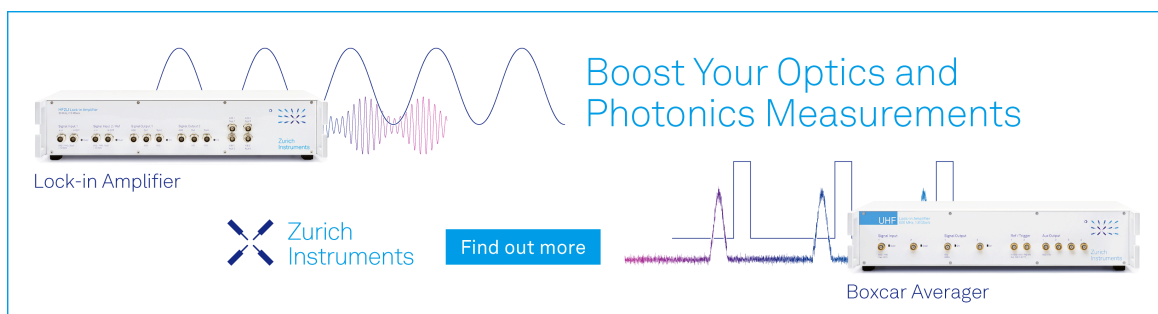
## More than little fragments of matter: Electronic and molecular structures of clusters **FREE**

Jarrett L. Mason; Carley N. Folluo; Caroline Chick Jarrold  



*J. Chem. Phys.* 154, 200901 (2021)

<https://doi.org/10.1063/5.0054222>



Boost Your Optics and Photonics Measurements

Lock-in Amplifier

Zurich Instruments

Find out more

Boxcar Averager

# More than little fragments of matter: Electronic and molecular structures of clusters

Cite as: J. Chem. Phys. 154, 200901 (2021); doi: 10.1063/5.0054222

Submitted: 15 April 2021 • Accepted: 9 May 2021 •

Published Online: 27 May 2021




View Online



Export Citation



CrossMark

Jarrett L. Mason, Carley N. Folluo, and Caroline Chick Jarrold<sup>a)</sup> 

## AFFILIATIONS

Department of Chemistry, Indiana University, 800 East Kirkwood Avenue, Bloomington, Indiana 47405, USA

<sup>a)</sup> Author to whom correspondence should be addressed: [cjarrold@indiana.edu](mailto:cjarrold@indiana.edu)

## ABSTRACT

Small clusters have captured the imaginations of experimentalists and theorists alike for decades. In addition to providing insight into the evolution of properties between the atomic or molecular limits and the bulk, small clusters have revealed a myriad of fascinating properties that make them interesting in their own right. This perspective reviews how the application of anion photoelectron (PE) spectroscopy, typically coupled with supporting calculations, is particularly well-suited to probing the molecular and electronic structure of small clusters. Clusters provide a powerful platform for the study of the properties of local phenomena (e.g., dopants or defect sites in heterogeneous catalysts), the evolution of the band structure and the transition from semiconductor to metallic behavior in metal clusters, control of electronic structures of clusters through electron donating or withdrawing ligands, and the control of magnetic properties by interactions between the photoelectron and remnant neutral states, among other important topics of fundamental interest. This perspective revisits historical, groundbreaking anion PE spectroscopic finding and details more recent advances and insight gleaned from the PE spectra of small covalently or ionically bound clusters. The properties of the broad range of systems studied are uniquely small-cluster like in that incremental size differences are associated with striking changes in stability, electronic structures, and symmetry, but they can also be readily related to larger or bulk species in a broader range of materials and applications.

Published under an exclusive license by AIP Publishing. <https://doi.org/10.1063/5.0054222>

## I. INTRODUCTION

With the development of increasingly sophisticated physical chemistry tools, both experimental and theoretical, that arose in the later part of the 1900s, the study of small fragments of matter with sizes of 2–10 atoms or molecules flourished. Nearly three and a half decades ago, Kaldor, Cox and Zakin, several of the earlier investigators of these species referred to as clusters, asked “How large does the cluster have to be before solid state theoretical description applies? What are the magnetic properties of “naked” and “dressed” clusters? Is there catalytic chemistry possible on such clusters, etc.?”<sup>1</sup> This exciting eruption of research was built on the seminal work by Moskovits and Hulse,<sup>2</sup> who co-deposited metal vapor and inert gases to create small fragments of matter. After many conferences, literature reviews, and compilations,<sup>3–9</sup> the motivation for cluster research goes beyond the discovery of enticing properties that might arise along the growth of matter from the atomic or single molecule limit to the bulk.

To set the stage, elemental and molecular clusters are typically separated in categories both by their size and by their binding

forces. Small clusters ( $1 < n < 100$  atoms) are commonly built atom-by-atom, or molecule by molecule, in a bottom-up approach and exhibit significant changes in properties such as ionization or bond dissociation energies with incremental increases in size. This punctuated variation in small cluster properties with size lies in contrast with nanoclusters, or nanoparticles, which are commonly formed by either synthetic bottom-up or mechanical top-down approaches. Nanocluster properties are affected by quantum confinement but exhibit a smooth evolution toward bulk properties upon addition of one atom or molecular unit, often with  $n^{-1/3}$ - or volume-dependence.

Within the small cluster category, another distinction lies in the bonding between constituent atoms or molecules. For example, water clusters,  $(\text{H}_2\text{O})_n$ , or clusters carrying an extra proton,<sup>10</sup> electron,<sup>11</sup> or some charged species<sup>12,13</sup> represent one of the more actively studied clusters<sup>14–16</sup> among the class of molecular clusters or ion–molecule complexes.<sup>17</sup> These and weakly bound systems such as helium clusters,  $\text{He}_n$ , are distinct from carbon clusters,  $\text{C}_n$ , or more ionic cluster such as metal oxides,  $\text{M}_x\text{O}_y$ , in which all constituent atoms are connected by a network of covalent and/or ionic

bonds. The latter of these has been commonly invoked as models for heterogeneous catalysts.<sup>18–63</sup>

As noted above, there have been several reviews to date on cluster studies. Examples include overviews on the use of vibrational spectroscopies for structure determination,<sup>64,65</sup> matrix-isolated metal clusters as models for heterogeneous catalysis,<sup>66</sup> general surveys of transition metal oxides,<sup>67</sup> transition metal cluster magnetic properties,<sup>68</sup> and metal cluster reactivity.<sup>69,70</sup> This perspective will focus on the application of anion photoelectron (PE) spectroscopy toward probing the electronic and molecular structures of “hard” clusters<sup>71</sup> and the interesting properties that arise in a range of systems. In simplest terms, anion PE spectroscopy involves photodetachment of a negatively charged cluster,  $M_n^-$ , and analysis of the energy of the resulting photoelectrons,



As will be detailed further below, the electron kinetic energies,  $e^- KE$ , reflect the energy between the initial anion state(s) and the final neutral state(s). We note here that some clusters are known to support doubly charged anionic states, despite the destabilization from intramolecular coulomb repulsion.<sup>72</sup> We will not consider dianions in this perspective, but they are a separate, interesting set of species.

Anion PE spectroscopy is particularly well-suited to cluster study. Figure 1 shows a schematic of the (a) simple direct detachment process in which a  $m/z$ -selected negative ion is photodetached, resulting in a neutral in a distribution of vibrational levels, with the

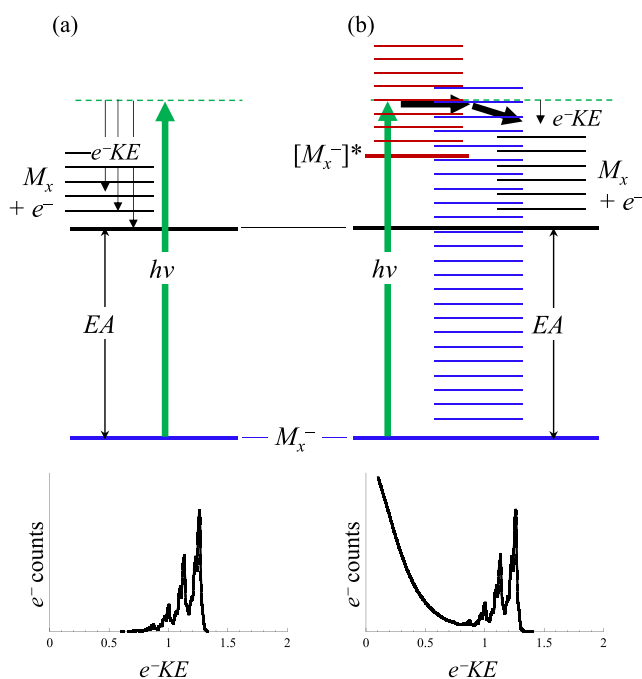


**FIG. 1.** Relative energy levels associated with direct detachment (a)  $M_x + e^- \leftarrow M_x^- + h\nu$  and an indirect/autodetachment pathway (b)  $M_x + e^- \leftarrow [M_x^-]^* \leftarrow M_x^- + h\nu$ . The representative spectra below indicate the expected transition intensities via direct detachment (Franck–Condon progression) and indirect detachment (high intensity at low  $e^- KE$ ) pathways.

total energy balanced by the  $e^- KE$  of the photoelectrons. The bottom panel shows the hypothetical distribution of  $e^- KE$  for a simple system in which a vibrational progression is resolved. As will be noted below, “hard” clusters can have complex electronic structures and therefore a high density of rovibronic levels of the anion that lie above the detachment limit, which can lead to indirect electron ejection processes. One such example is shown in Fig. 1(b): The incident photon is resonant with such an excited level of the anion, which can lead to internal conversion to a very high vibrational level of the anionic ground state and electron loss through thermionic emission, which favors low  $e^- KE$  statistically.

An additional powerful feature of anion PE spectroscopy is the ability to map the low-lying electronic structures of neutral clusters, which provides a view of the evolution of electronic structure as a function of cluster size and composition. Figure 2 schematically illustrates how the evolution of the electronic structure of small

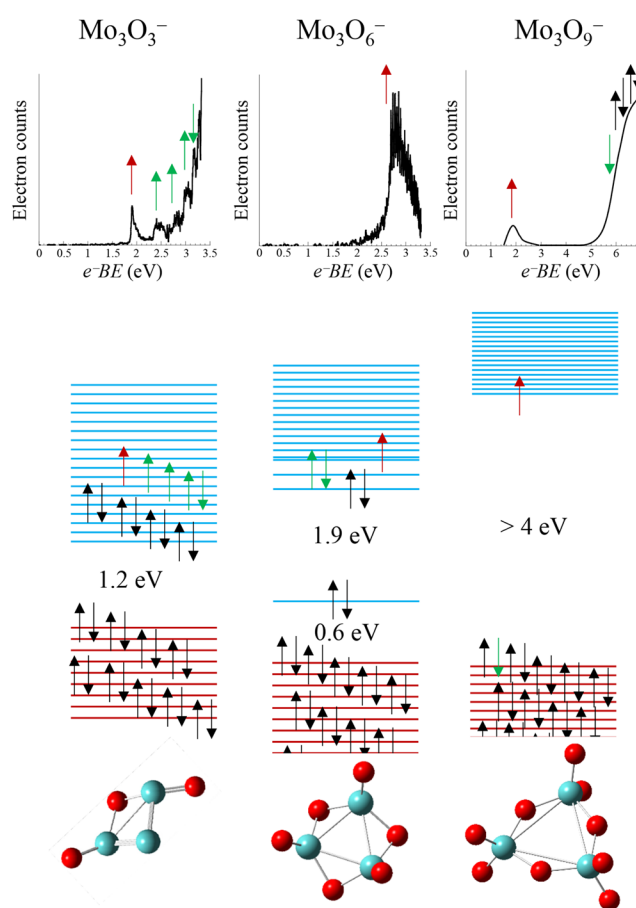


**FIG. 2.** Illustration of the evolution of the electronic structure of a small group Mo-oxide clusters ( $\text{MoO}_3$  bulk stoichiometry, bandgap  $\sim 3.0$  eV) as oxidation increases from  $\text{Mo}_3\text{O}_3$  to  $\text{Mo}_3\text{O}_6$  and to  $\text{Mo}_3\text{O}_9$ . The red horizontal lines represent relative energies of the fully occupied orbitals described as predominantly O 2p orbitals (correlating to the bulk valence band). Blue horizontal lines represent Mo-local 4d and 5s orbitals (correlating to the bulk conduction band). Arrows indicate electronic occupancy; “red” electrons indicate the excess electron in the anion associated with the lowest energy detachment transition, with “green” electrons indicating other accessible detachment transitions.

metal oxide clusters, such as  $\text{Mo}_3\text{O}_y^-$ , from undercoordinated (sub-oxide) to fully oxidized (bulk stoichiometric) can be probed using anion PE spectroscopy. As with bulk  $\text{MoO}_3$ , the clusters have mixed ionic/covalent character. The red horizontal lines represent orbitals predominantly described as O 2p orbitals, which have some covalent overlap with the Mo 4d orbitals; these orbitals correlate with the valence band of bulk  $\text{MoO}_3$ . The turquoise lines represent the metal-local 5s and 4d orbitals that correlate with the bulk conduction band. Anion PE spectroscopy accesses neutral states via detachment of electrons from the highest lying valence orbitals. In this simple illustration, the “red” electron is the excess electron in the anion, which is in the highest occupied orbital and “green” electrons can additionally be detached with a ultraviolet (UV) or visible photon. In suboxides, multiple valence electrons occupy the Mo-local orbitals. Because they are energetically close-lying, the PE spectrum will show multiple overlapping transitions associated with, for example, the detachment of the “red” and “green” electrons, with differences in the  $e^-KE$  values associated with the different final states equaling the energy difference between the close-lying states. For example, the PE spectrum of  $\text{Mo}_3\text{O}_3^-$  exhibits at least five overlapping transitions within a narrow energy range. The spectrum becomes less congested with transitions as the number of electrons occupying the crush of metal orbitals decreases to the point of the stoichiometric cluster. Note that in the stoichiometric  $\text{Mo}_3\text{O}_9^-$  cluster, the PE spectrum of which is shown hypothetically based on the spectrum of the  $\text{W}_3\text{O}_9^-$  congener,<sup>73</sup> the energy difference between the two lowest energy detachment transitions reflects the bulk analog of the HOMO–LUMO gap!

The electron affinity represents the relative stability of the anion and neutral, which reflects a particular stability of open or closed shell electronic structures, physical stability of the structure, etc. Therefore, neutral clusters with particularly stable structures can have relatively low electron affinities.

As noted above, charged clusters are readily  $m/z$ -selected prior to photodetachment measurements. However, mass selectivity is not a unique advantage to anion PE spectral studies. Charged clusters are common targets of reactivity studies that probe the size and composition-dependent chemical properties, and many of the studies on cluster models for catalysis noted above implement mass selection of cluster reactants, products, or both. Collision induced dissociation in guided ion beams,<sup>74,75</sup> which can measure the bond energies as a function of size and composition, can identify clusters with particular stabilities and can be extended to measure the melting temperatures of clusters as a function of size.<sup>76</sup> Vibrational and electronic action spectra also leverage the mass selectability of chromophore and mass analysis of daughter ions.<sup>77,78</sup>

## II. METHODS

The general experimental strategy for measuring anion PE spectra of negative ions is to couple a cluster ion source to a mass spectrometer or mass filter. The photodetachment laser is then intersected with the ion beam of a selected  $m/z$ , and the photoelectron kinetic energy distribution is measured. The success of this general approach to cluster study is in no small part reliant on the computational characterization of potential molecular and electronic structure characterization, which shall be discussed briefly in

Sec. II C. Following is a survey of several approaches taken to anion PE spectroscopic interrogations of “hard” clusters.

### A. Cluster sources

Different strategies for cluster production have been formulated over the years. Metal cluster production techniques, including seeded oven sources, sputtering sources, liquid–metal ion sources, and laser vaporization sources, were reviewed by de Heer in 1993.<sup>7</sup> As the PE spectrometers have used both continuous wave (CW) and pulsed lasers to photodetach the negative ions, both CW and pulsed cluster sources have been used in the studies surveyed in this perspective.

Lineberger, whose seminal PE spectroscopy studies implemented CW lasers, developed a flowing afterglow ion source by cathodic sputtering from a DC discharge.<sup>79,80</sup> In a pulsed variation, the pulsed arc cluster ion source (PACIS) introduced by Meiwes-Broer and co-workers used high voltage discharge coinciding with a pulse of high-pressure buffer gas to produce a wide range of clusters of the material of the metal electrodes.<sup>81,82</sup>

Smalley<sup>83</sup> and Bondybey<sup>84</sup> simultaneously developed laser ablation sources using bulk targets made of the desired cluster material. The Smalley-style source coupled a pulsed molecular beam valve in close proximity to the ablation spot on the target, with a high-pressure pulse of helium issued from the valve entraining the metal vapor generated by ablation, which allowed for the production of larger, internally cold clusters. Laser ablation targets include bare metal rods, pressed pellet targets, liquid metal targets, and powder-coated rods.<sup>85–88</sup> A schematic of a Smalley-type source used in our laboratory<sup>89</sup> is shown in Fig. 3(a). Several variations of this cluster source and their applications are included in a review by Duncan,<sup>36</sup> and cluster sources featuring two separate ablation targets for controlled production bimetallic clusters have been detailed.<sup>90,91</sup> A variety of ns pulsed lasers have been used in ablation sources, although femtosecond lasers may increase the cluster sizes produced.<sup>92–94</sup> Ablation sources generate a mixture of cation, anion, and neutral cluster species with varying compositions for different charged species, making  $m/z$  selection essential.<sup>37</sup>

Production of ligated clusters has been achieved by several groups using a two-valve scheme in which one valve introduces a high-pressure buffer gas that sweeps over the plasma generated by ablation of a target to produce the clusters, while a second valve injects a ligating compound downstream of the point of ablation, giving clusters time to coalesce and cool.<sup>95</sup>

Wet-synthesized ligated clusters can also be introduced into the gas phase. For example, a high flux cluster beam source developed by Palmer and co-workers is operated by sputtering metal cluster ions from a matrix.<sup>67,68</sup> More recently, Wang and co-workers brought cryogenically cooled ion traps into common use in anion PE spectroscopy studies and beyond.<sup>96</sup> These traps can couple CW sources such as electrospray ionization (ESI) sources into a pulsed mass spectrometer [e.g., Fig. 3(b)] by using ion traps that accumulate ions, injecting them then into a pulsed mass spectrometer at the experimental repetition rate. This approach can also be applied to laser ablation sources, typically to cryogenically cool ions in the trap prior to spectroscopic investigation. The clear advantage of coupling an ESI source is the ability to introduce clusters generated via benchtop synthetic methods.

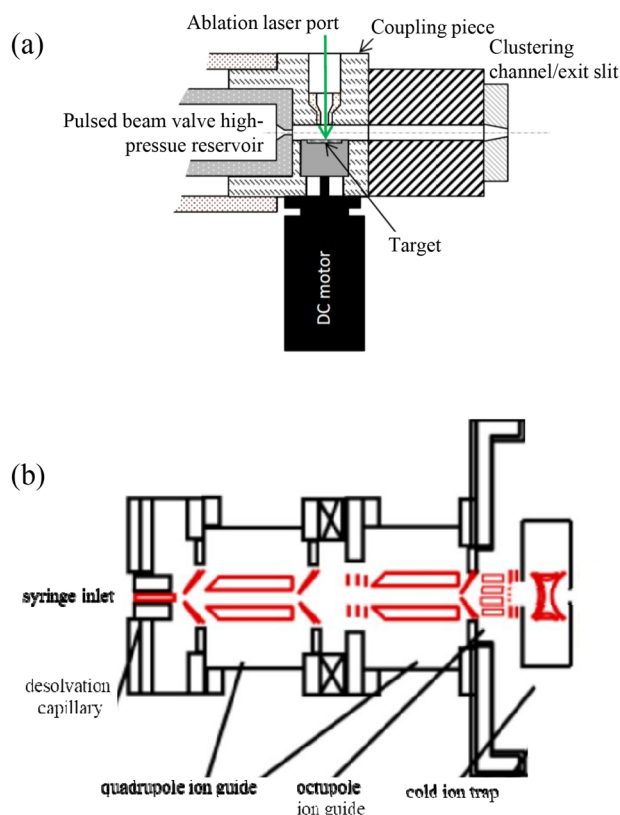


**FIG. 3.** Representative cluster sources: (a) the pulsed “Smalley-style” source that uses laser ablation of a target material coupled with a pulsed molecular beam valve described in Ref. 89 and (b) a CW style ESI/ion trap source for introducing bench-top synthesized clusters into the gas phase. Reproduced with permission from Wang, *J. Chem. Phys.* **143**, 040901 (2015). Copyright 2015 AIP Publishing LLC.

## B. Photodetachment and $e^-KE$ analysis

Depending on whether the source is pulsed or CW, the mass selection component is a time-of-flight or quadrupole mass spectrometer or a Wien filter.<sup>97</sup> In either case, with a mass-filtered CW or pulsed anion beam, the anions are intersected and selectively photodetached with a fixed-frequency laser as per Eq. (1), yielding neutrals in a distribution of electronic, vibrational, and rotational states and photoelectrons in a distribution of kinetic energies,  $e^-KE$ , per

$$e^-KE = h\nu - EA - E_{e,vib,rot}^{neutral} + E_{e,vib,rot}^{anion}. \quad (2)$$

If the anionic precursors are internally cold (a valid assumption for ions that have been cryogenically trapped, *vide supra*, is that  $E_{e,vib,rot}^{anion} \approx 0$ ), the  $e^-KE$  distribution will reflect the energies of rovibronic states of the neutral relative to a single level of the anion. In general, one-electron transitions are the most intense, and  $\Delta s = \pm 1/2$ . There are notable exceptions to this rule.

The  $e^-KE$  values for any given transition are photon energy dependent. However, PE spectra are typically reported in terms of the photon energy-independent binding energy,  $e^-BE$ , related via

the simple relationship

$$e^-BE = h\nu - e^-KE, \quad (3)$$

which allows for direct comparison of spectra collected with different detachment photon energies.

Photoelectrons generated from a randomly oriented ensemble of anions have angular distribution relative to the electric field vector of the laser described by the following equation formulated by Cooper and Zare:<sup>98</sup>

$$\frac{\partial\sigma}{\partial\Omega} = \frac{\sigma_{total}}{4\pi} \left[ 1 + \beta(E) \left( \frac{3}{2} \cos^2\theta - \frac{1}{2} \right) \right], \quad (4)$$

where  $\theta$  is the angle between the direction of the ejected electron and incident photon polarization,  $\sigma_{total}$  refers to the total cross section, and  $\beta$  is an asymmetry parameter, ranging in value from 2 to  $-1$ . The asymmetry parameter in atomic systems is a function of the angular momentum,  $\ell$ , of the outgoing photoelectron wave, which relates to the atomic electronic orbital of origin via conservation of angular momentum. That is, detachment of an electron from an s-orbital yields photoelectrons with  $\ell = 1$  and p-orbitals yield  $\ell = 0, 2$ . For molecules with less-than-spherical symmetry, the relationship is less straightforward; an elegant and physically insightful description of the relationship between the outgoing photoelectron waves and the molecular orbitals of origin has been provided by Sanov.<sup>99</sup>

The methods of electron kinetic energy analysis in CW experiments implement tools such as hemispherical energy analysis,<sup>100</sup> while in pulsed experiments, photoelectron time-of-flight, either in a magnetic bottle or in a field-free drift tube, has been in common use along with photoelectron imaging.<sup>101</sup> A comparison of these three types of electron detection methods is shown in Fig. 4. Both the hemispherical analyzer and field-free time-of-flight have low collection efficiency. The magnetic bottle time-of-flight approach, which has 100% collection efficiency, typically has a lower duty cycle (e.g., 10 Hz) although recent developments in electron trapping offer higher duty cycles, e.g., with synchrotron radiation facilities.<sup>102</sup>

A particularly creative and powerful combination of ion source and anion PE spectroscopy was demonstrated by Kappes and coworkers, who coupled an electrospray source to an ion mobility spectrometry setup, which allowed structural isomer separation of a particular  $m/z$  prior to interrogation using a magnetic bottle anion PE spectrometer.<sup>103</sup> As will be noted below, competitive structural isomers of clusters frequently co-exist in small- to mid-sized elemental clusters and metal oxide clusters in lower-than-traditional oxidation states.

Photoelectron imaging, which was brought into broader use in the anion PE spectroscopy community by Sanov,<sup>104</sup> leverages a technique developed in pioneering work by Chandler and Houston based on a design of Eppink and Parker.<sup>105</sup> A great advantage of this technique is the simultaneous measurement of electron kinetic energy (via velocity) and angular distributions as the 3D electron cloud is projected onto a 2D surface. Attending this capability is the added ability to probe indirect detachment pathways that affect photoelectron angular distributions, such as autodetachment.<sup>106,107</sup>

The push to higher resolution photoelectron imaging has made it a powerful tool for studying a broader range of anionic systems.<sup>108,109</sup> Slow electron velocity imaging (SEVI)<sup>110,111</sup> has emerged as a more reliable and broadly applicable version of high-resolution

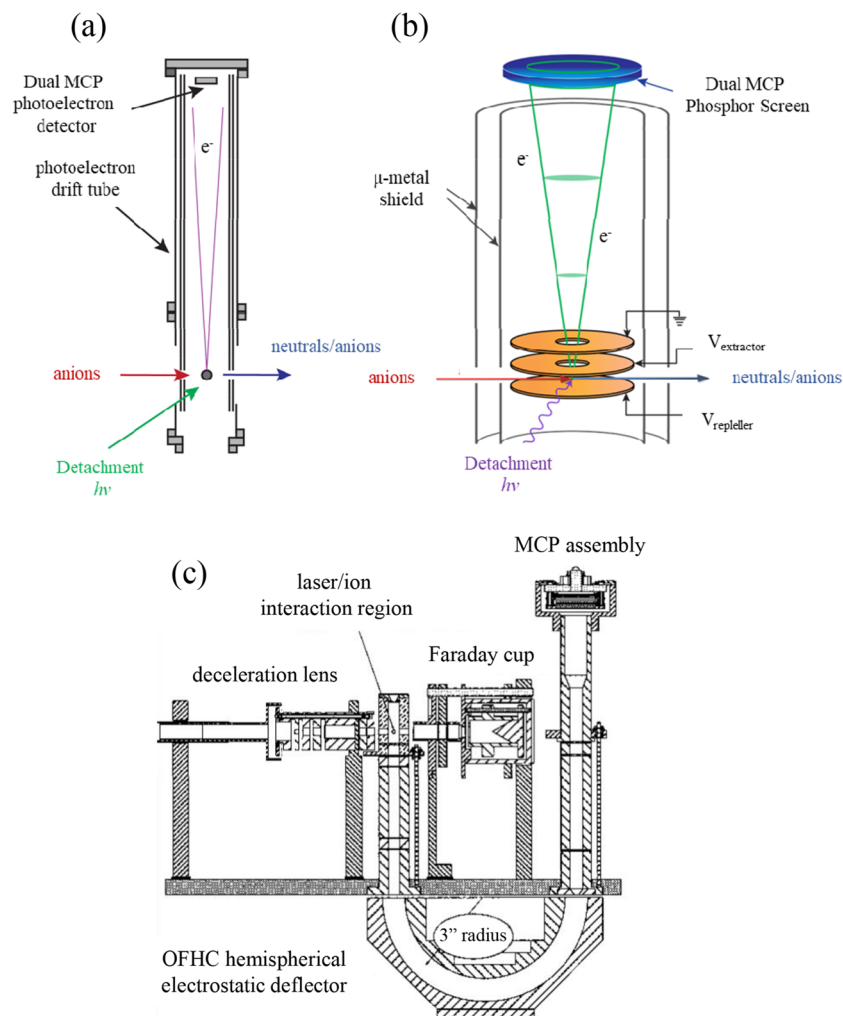


**FIG. 4.** Representative electron detection schemes: (a) the field-free time-of-flight drift tube used to measure drift times of the fraction of photoelectrons that reach the detector (introducing a magnetic bottle scheme allows 100% collection efficiency), (b) the velocity map imaging setup that uses extractors and repellers to project the 3D electron cloud onto a 2D phosphor screen, and (c) the hemispherical analyzer in which only electrons of a specific kinetic energy are allowed to pass and reach the detector. Modes (a) and (b) are used in pulsed experiments, and mode (c) is typically used in CW experiments. (c) Reproduced with permission from Travers *et al.*, *J. Chem. Phys.* **111**, 5349 (1999). Copyright 1999 AIP Publishing LLC.

PE spectroscopy than zero electron kinetic energy (ZEKE) spectroscopy of anions, the latter of which involved tuning through the detachment continuum and discriminating against the detection of photoelectrons with greater than near-zero kinetic energy.<sup>112</sup> Anion ZEKE was limited to the study of detachment transitions yielding  $\ell = 0$  photoelectrons, i.e., with non-zero detachment cross sections per the Wigner threshold law,<sup>113</sup>

$$\sigma \propto \sigma_0 (E_{hv} - E_{\text{threshold}})^{\ell + \frac{1}{2}}. \quad (5)$$

In SEVI experiments, similarly, the photon energy is held anywhere between 0.01 and 0.5 eV above the detachment threshold; at each wavelength, a high-resolution photoelectron spectrum is obtained for a limited  $e^- KE$  range and a complete spectrum may be stitched together.<sup>114–116</sup> While ZEKE generally suffers from grueling collection times, SEVI has a high collection efficiency and maintains the measurement of photoelectron angular distributions.<sup>117</sup>

Ultrafast anion PE spectroscopy<sup>118–120</sup> has been conducted on a number of cluster systems to follow the evolution of anionic states with time. As a one-photon detachment tool, ultrafast lasers do not

offer an advantage over CW or nanosecond lasers. However, in a time-resolved pump-probe setup, dynamics of excited electronic states can be measured. In this technique, one photon drives an excitation, and the second photon detaches the time-evolving cluster anion. This technique has been used to explore the intermolecular dynamics in soft clusters, e.g., dihalide anions solvated by a finite number of CO<sub>2</sub> molecules, or electronic relaxation in metal clusters. Excellent reviews of this now mature technique were presented by Stolow *et al.*<sup>121</sup> and Fielding and co-workers.<sup>122</sup>

### C. Computational spectroscopy

A thorough survey of computational methods that have supported anion PE spectroscopic studies of clusters is beyond the scope of this perspective. However, it is important to note that a more detailed and insightful picture of the properties of clusters can be gained from reconciling experimental spectra with computational results on the anionic and neutral species. Without a general starting point in terms of which cluster electronic and molecular structures are viable for consideration, assignment of spectra is limited to

very low-order interpretation, as small covalently or ionically bound clusters can potentially form numerous different structures.

Identifying viable stable structures and wavefunctions without *a priori* knowledge of the structures can be achieved using a variety of approaches to global minimum energy searches, a number of which have been summarized by Jian *et al.*<sup>123</sup> Density functional theory (DFT) calculations with or without single-point calculations conducted at more accurate (and expensive) levels are commonly used for structure optimization using a range of quantum chemistry packages.<sup>124</sup> Calculations readily provide zero-order spectroscopic parameters to compare the spectra: The difference in the zero-point corrected total energies of the global minimum energy neutral and anion corresponds to the adiabatic electron affinity, which often, but not always, corresponds to the lowest  $e^-BE$  origin of the experimentally observed transitions. This does not apply to situations in which the lowest energy isomer of the anion has zero Franck–Condon overlap with the neutral (e.g., the anion and neutral favor very different molecular structures) or if the transition between similar structures is not one-electron allowed.

Similarly, it is straightforward to calculate the energy of the neutral cluster confined to the structure of the anion. The energy difference corresponds to the vertical detachment energy, which is the  $e^-BE$  at which the intensity of an electronic transition reaches a maximum (highest Franck–Condon overlap). Time-dependent DFT can help in assigning excited state transitions observed in the spectra.

More definitive structural assignments can be made with spectral simulations based on more detailed spectroscopic parameters determined from the differences between the initial anion and final neutral states, the respective vibrational frequencies, and normal coordinates. Simulations that calculate Franck–Condon overlaps between the anion and neutral vibronic levels provide a more detailed vibronic profile of detachment transitions. Home-written codes, such as the one developed in our own group,<sup>125</sup> can convolute stick spectra with the  $e^-KE$ -dependent experimental resolution and allow for different “temperatures” associated with different vibrational modes. This control takes into account the non-equilibrium conditions in some cluster sources in which lower-frequency modes can cool more efficiently than higher-frequency modes. Of course, simulations are most helpful when vibrational features are resolved in the associated anion PE spectra, which is not always the case, particularly with larger clusters. Other open access spectral simulations programs such as ezFCF (formerly ezSpectrum) and ezDyson are also widely used for simulating experimental PE spectra.<sup>126</sup>

Useful constructs from the computational studies of anion and neutral states are Dyson orbitals,<sup>127,128</sup> which allow visualization of the difference between the  $N$ -electron state and the  $N - 1$  electron state, and Natural Ionization Orbitals (NIOs), which add insight into electronic relaxation associated with the final  $N - 1$  state.<sup>129</sup> The latter can further be used to calculate the photodetachment cross sections and PADs of transitions using standard DFT model chemistries.<sup>130</sup> For systems with multiple close-lying photodetachment transitions, this additional information can enrich the spectral assignments and the overall picture of the cluster electronic structure. In very simple terms, the NIO picture can provide a contrast between electron detachment transitions that can be described as purely one-electron and more complex detachment processes. Examples of both are shown in Fig. 5. In the case of the Ce-doped

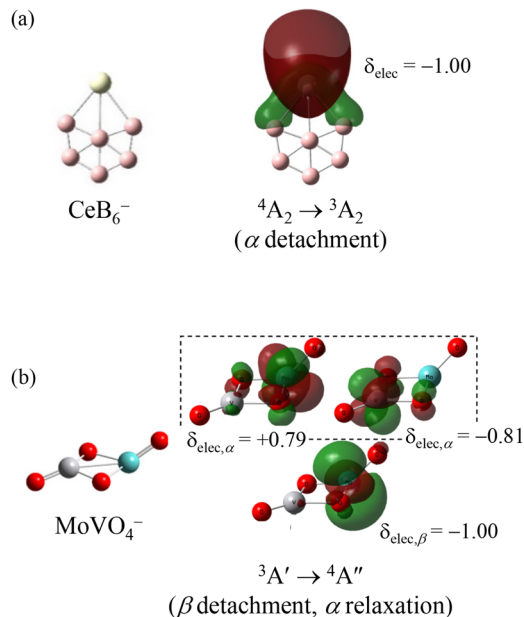


**FIG. 5.** NIO visualizations of the orbital vacated by a photoelectron (a) for the case of a purely one-electron transition predicted for the Ce (cream)-doped  $B_6$  (pink) cluster anion [Ref. 131] and (b) in the  $3A' \rightarrow 4A''$  transition in  $MoVO_4^-$ —better characterized as a two-electron process involving detachment of an electron localized from an orbital localized on the Mo (turquoise) center and relaxation of an electron from the V center (gray) to the Mo center, shown in the dashed box (Ref. 132). O atoms are indicated in red. Adapted with the permission from (a) Mason *et al.*, *J. Phys. Chem. A* **123**, 2040 (2019). Copyright (2019) American Chemical Society, and (b) Thompson *et al.*, *J. Chem. Phys.* **146**, 104301 (2017). Copyright 2017 AIP Publishing LLC.

$B_6$  cluster anion [Fig. 5(a)],<sup>131</sup> the detachment process can be visualized as creating a hole in the orbital situated on the Ce center, while in the case of the heterometallic  $MoVO_4^-$  cluster [Fig. 5(b)],<sup>132</sup> the transition between from the  $3A'$  anionic ground state to the  $4A''$  neutral ground state, which was relatively very low in intensity in the experimental spectrum, can be described as detachment accompanied by significant relaxation of a remaining metal-local electron.

### III. ANION PE SPECTRA OF CLUSTERS ACROSS THE PERIODIC TABLE

While it would be nearly impossible to fully account for the prolific output of anion PE spectroscopic studies conducted on “hard” clusters, this perspective will survey several noteworthy and representative studies, both foundational and more recent. The studies are organized in terms of the type of clusters, classified as pure elemental, mixed (e.g., ionic, metal oxides, otherwise mixed elemental clusters), doped (clusters of predominantly one element with a single atom of a different element), and ligated clusters.

#### A. Elemental clusters

Anion PE photodetachment techniques have been applied toward the study of elemental clusters across the Periodic Table from the alkali metals<sup>133</sup> to  $I_3^-$  (though this molecule is considered

a reaction intermediate rather than a “hard” elemental cluster)<sup>134</sup> and down to the f-block elements.<sup>135</sup> Starting this particular section in the p-block, early work on carbon clusters was driven by their importance in astrochemistry and combustion.<sup>136</sup> A review dedicated to carbon clusters, their size evolution, and the discovery of C<sub>60</sub> and carbon nanotubes would be encyclopedic in size.

In addition to anion PE and ZEKE spectral studies of small carbon clusters, studies on heavier group IV elemental clusters of silicon,<sup>137–139</sup> germanium,<sup>140,141</sup> tin,<sup>142,143</sup> and lead<sup>144,145</sup> have revealed the fundamental connection between cluster and bulk properties. In particular, the persistent low-dimensionality of carbon clusters is related to the unique stability of  $\pi$  bonding in carbon, a property behind the stability of graphite, while the energetic accessibility of unoccupied *nd* orbitals of the group IV elements leads to the formation of three-dimensional clusters in the very small size regime. This effect is reflected very plainly in the spectra. Figure 6 shows the anion PE spectra of odd-numbered carbon<sup>146</sup> and tin clusters for comparison. The near-vertical appearance and systematic increase in electron binding energy with the size for the carbon clusters reflect the nearly identical linear structures for both the anion and neutral, and stabilization from charge delocalization with increasing chain length leads to higher binding energies. In contrast, the more compact 2D (in the case of Sn<sub>3</sub><sup>-</sup>) and 3D structures of small tin clusters result in multiple, close-lying, and vibrationally broadened electronic transitions. Relativistic effects become more important with the heavier elements, with spin-orbit splitting competing with Jahn–Teller effects in governing cluster structures, such as Sn<sub>3</sub>.<sup>143</sup> While Si and Ge clusters were not found to form cage structures known for several magic C<sub>*n*</sub><sup>-</sup>/C<sub>*n*</sub> clusters, Sn<sub>12</sub> and Pb<sub>12</sub> were found to form stable, icosahedral structures.<sup>142,144</sup> Related to this high-symmetry molecular character, Pb<sub>12</sub><sup>-</sup>, studied by VUV

PE spectroscopy,<sup>147</sup> showed non-metallic behavior, as evidenced by the low screening of a core hole. Metallic behavior emerged for *n* > 20.

In contrast to group IV elements, the p-block neighbors, nitrogen and oxygen, are in gas phase at standard temperature and pressure. N<sub>2</sub> does not bind an electron, but O<sub>2</sub> does. O<sub>4</sub><sup>-</sup> is a very complex, thoroughly investigated molecular anion in which the charge is shared between two O<sub>2</sub><sup>1/2-</sup> molecules.<sup>148–150</sup> Larger oxygen clusters tend to be described as “soft” [O<sub>4</sub><sup>-</sup>](O<sub>2</sub>)<sub>*n*</sub> clusters. The heavier group V<sup>151,152</sup> and VI<sup>153</sup> elements have been among the earlier clusters that were studied by this community.

Boron has inspired interest because of applications in high energy density storage materials and graphite/graphene alternatives. Boron’s one-electron deficiency compared to neighboring carbon imbues these clusters with interesting electronic properties, particularly with the boron cluster propensity for establishing aromaticity. Bowen reported early foundational work on boron clusters;<sup>165</sup> since then, prolific boron cluster studies<sup>154</sup> by Wang and co-workers have been at the forefront of boron cluster research, exploring exciting planar, vacancy-punctuated hexagonal structures, puckered structures, borospherenes with interesting electronic structures,<sup>155</sup> and dopant atom effects,<sup>156</sup> with cluster sizes well into the nanomaterial regime.<sup>157</sup>

Situated below boron, aluminum clusters are also worth a comment, having been studied by anion PE spectroscopy by several groups over the past few decades.<sup>158–161</sup> Early studies were partly motivated by the seminal findings on apparent spherical shell-closing patterns of alkali metal clusters from abundance spectra, modeled within the jellium picture of a uniformly positive sphere supporting electrons.<sup>162</sup> The question of whether aluminum clusters could similarly be modeled by the jellium picture arose in the early

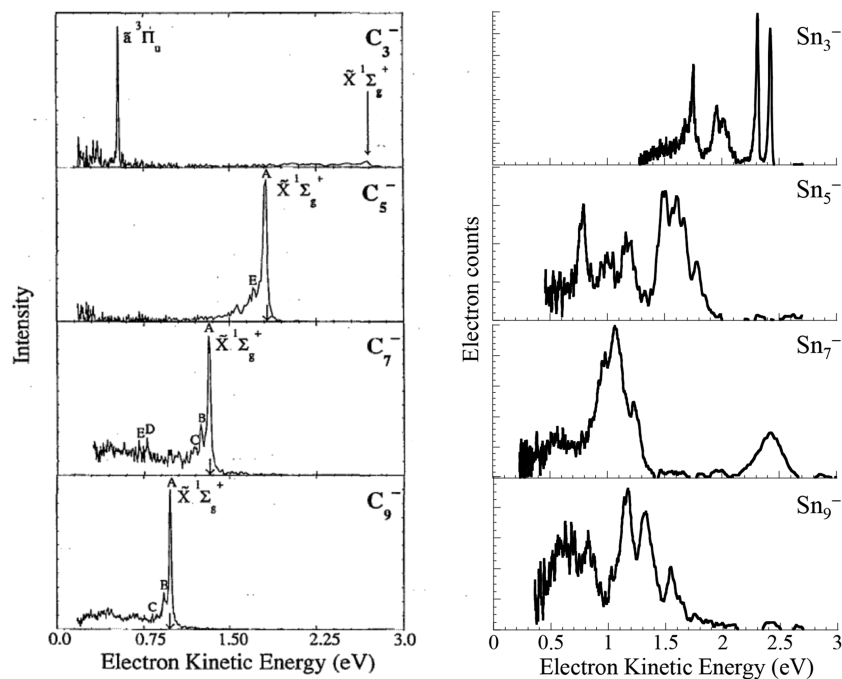


**FIG. 6.** Comparison of the anion PE spectra of two series of group IV clusters obtained using 4.66 eV photon energies (except in the case of Sn<sub>3</sub><sup>-</sup>, which was obtained with 3.495 eV, but the *e*<sup>-</sup> KE values are set to 4.66 eV - *e*<sup>-</sup> BE for direct comparison). Linear carbon cluster anions (Ref. 146) exhibit near-vertical electronic transitions to linear neutral clusters (odd-numbered clusters shown; even-numbered cluster spectra are similar but have systematically higher EAs), while tin cluster anions form two- or three-dimensional structures with numerous close-lying electronic states (Ref. 143). C<sub>*n*</sub><sup>-</sup> spectra reproduced from Arnold *et al.*, J. Chem. Phys. **95**, 8753 (1991). Copyright 1991 AIP Publishing LLC and Sn<sub>*n*</sub><sup>-</sup> spectra adapted with the permission from Moravec *et al.*, J. Chem. Phys. **110**, 5079 (1999). Copyright 1999 AIP Publishing LLC.



1990s.<sup>163</sup> The combination of anion PE spectroscopy and higher-level calculations did show the jellium electronic shell structure for several of the clusters, highlighting the punctuated evolution of cluster properties in the small cluster size regime and underscoring the enhanced fundamental understanding that can be gleaned by intimate coupling between experimental and computational efforts.<sup>164</sup> In a number of studies,  $\text{Al}_{13}^-$  was found to be a particularly stable species and exemplary of a superatom.<sup>165–171</sup> Superatoms are defined as small, stable, and compact clusters with quantum states resembling the electronic orbitals in atoms. Examples of mixed-elemental clusters exhibiting superatom character are included below.

Transition metal clusters, beyond the heavier p-block metal elemental clusters, present a different level of complexity in terms of electronic structures due to partially filled  $nd$  orbitals.<sup>4</sup> They were also among the first elemental clusters studied by anion PE spectroscopy.<sup>172–175</sup> Of particular interest in earlier studies was the evolution of band structure and metallic behavior,<sup>176</sup> but they also offered an enticing window into the evolution of magnetic properties. As noted above, anion PE spectroscopy can directly map the high density of electronic states evocative of metallic behavior.<sup>177</sup> Because of the fundamental inseparability of electronic and molecular structures, using the combination of theory and PE spectroscopy to determine molecular structures has also been a productive approach.

While inert as bulk, small supported gold nanoparticles have demonstrated a range of catalytic activity,<sup>178</sup> which had augmented the motivation for exploring the electronic and molecular structures of small gold clusters. Wang and co-workers explored a range of gold clusters,<sup>179</sup> the smallest of which assume planar (2D) structures. They demonstrated a transition from 2D to 3D structures at  $n = 12$ , with  $\text{Au}_{12}^-$  found to coexist in both 2D and 3D structures.<sup>180–183</sup> Planar structures, rather than 3D structures for the smaller gold clusters, were rationalized by  $5d$ – $6s$  hybridization enabled by relativistic effects.<sup>184</sup> Larger gold clusters, e.g.,  $\text{Au}_{26}^-$ , also studied by Wang and co-workers have been shown to have several energetically competitive molecular architectures that coexist experimentally, including core–shell, cage, tubular, and hexagonal motifs, as illustrated in Fig. 7, which shows four structures identified computationally that appear to contribute to all the observed PE spectrum of  $\text{Au}_{26}^-$ .<sup>182</sup> The structural diversity has been similarly confirmed by the studies of Kappes and co-workers, who have employed electron diffraction in their studies of trapped and size-selected gold cluster anions<sup>185</sup> in addition to numerous other metallic systems.<sup>186,187</sup>

Direct detachment transitions can generally be treated as instantaneous one-electron processes in simple molecules, but this description is not necessarily appropriate when considering more complex metal clusters, and the high density of electronic states in the neutral suggests the same of the precursor anions. Early evidence of this was seen in the form of thermionic emission in the PE spectra of small tungsten<sup>188</sup> and other<sup>189</sup> cluster anions. As illustrated in Fig. 1(b), thermionic emission occurs when the anion is photoexcited to another higher-lying anionic state, followed by interconversion to a high vibrational level of the ground state of the anion, whereupon the electron is ejected. Because electron ejection follows the initial excitation event, the photoelectron angular distribution of thermionically emitted electrons is isotropic.<sup>190</sup> Thermionic emission from bulk emitters is statistical, and  $W_n^-$  clusters exhibit

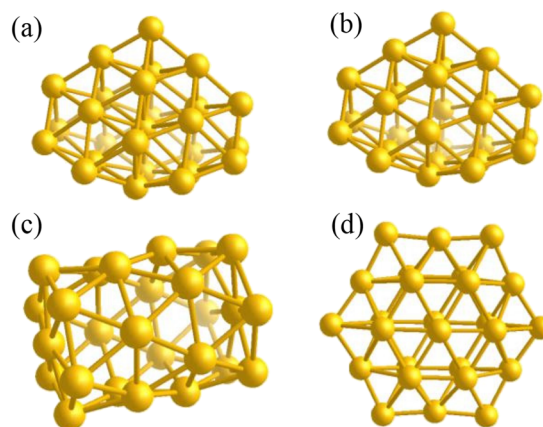


FIG. 7. Energetically competitive structures of  $\text{Au}_{26}^-$  (Ref. 182). The variation in structure underscores the fluxionality of the metallic gold cluster anions. Reprinted with permission from Schaefer *et al.*, ACS Nano, **8**, 7413 (2014). Copyright 2014 American Chemical Society.

statistical thermionic emission in clusters as small as  $n = 4$ . A different indirect detachment process frequently encountered in anion photodetachment spectroscopies is autodetachment in which ejection of an electron by a long-lived (*ca.* ps) rovibrationally excited quasibound state of the anion is observed to follow propensity rules associated with electronic, vibrational, or rotational relaxation to the final neutral state, with the ejected electron having a discrete kinetic energy associated with the relaxation. This process, which has been observed in a number of soft cluster studies, will not be described further here.

The high density of electronic states in transition metal clusters also opens the door to the study of the dynamics of excited electronic states of cluster anions, which have been measured using time-resolved PE spectroscopic techniques. In simple terms, a pump laser excites the cluster anion to an excited, bound, or quasibound electronic state, and the evolution of that excited state is probed by a delayed second pulse, which detaches the electron allowing the measurement of the PE spectrum of the clusters from the evolving excited state. The appearance of the PE spectrum changes with the delay between the excitation and detachment pulses.

Using ultrafast anion PE spectroscopy, evidence of non-metallic behavior in small Pb cluster anions was observed: Despite the density of electronic states at larger cluster sizes, picosecond relaxation times suggested non-metallic behavior,<sup>191</sup> up to and including  $\text{Pb}_{38}^-$ , which showed a remarkable polarizability difference than the elemental bulk. Similarly, intra- and inter-band excitations in  $\text{Hg}_n^-$  clusters have been explored by Neumark and co-workers.<sup>119,120</sup> These clusters are, on the one hand, very simple, with each atom contributing a  $5d^{10} 6s^2 1S_0$  electronic structure, resulting in a fully occupied  $6s$  “band,” with a single electron in the  $6p$  “band” in the cluster anion. They were able to discern three different time-dependent processes, including  $6s \rightarrow 6p$  interband excitation with Auger ejection,  $6s \rightarrow 6s$  intraband excitation, with time-evolving detachment of the excited state, and  $6s \rightarrow 6p$  excitation with time-evolving detachment of the directly excited electronic state. Lifetimes were dependent on the cluster size. In sum, these experiments

offer deep insight into the evolution of band structures with cluster size.<sup>192</sup>

Koop *et al.* employed ultrafast anion PE spectroscopic studies of a range of elemental clusters, including p-block and transition metal clusters, in the search of long-lived excited electronic states.<sup>193</sup> They made the curious observation that only cluster anions accompanied by spectra with narrow features had lifetimes on the ps timescale. The rationale was that narrow features reflected low coupling between the molecular and electronic structures, which suggests non-bonding character of the orbitals associated with the excitation.

Time resolved PE spectroscopy of “hard” clusters such as those described above has not been as commonly adopted as it has been for “soft” clusters, many of which are relevant in biological charge transfer or radiation damage processes.<sup>194</sup>

## B. Ionic clusters, metal oxide clusters, and other binary and higher-order clusters

If one of the original curiosities surrounding elemental clusters was the size at which bulk properties began to emerge, one of the questions arising in metal oxides or other ionic clusters was how the localized bonding in the bulk materials would be reflected in small clusters. In addition, small clusters offer a platform for studying non-stoichiometric species. For example, our laboratory has extensively characterized numerous metal oxide clusters, both homo-<sup>195–198</sup> and heterometallic,<sup>199–203</sup> in lower-than-traditional oxidation states (suboxides).

One of the earliest studies on ionic clusters was reported by the Bowen group, who demonstrated the slow evolution toward bulk F-center energy in  $(\text{CsI})_n^-$  clusters.<sup>204</sup> These stoichiometric clusters have low electron affinities, unlike the incrementally non-stoichiometric alkali halide  $(\text{MX})_n\text{X}^-$  clusters, which have electron binding energies higher than the bare  $\text{X}^-$  halide anion. The work by Bowen on the stoichiometric clusters showed a smooth  $n^{-1/3}$  dependence on binding energy, which is what is expected in a simple quantum confinement picture, suggesting that the sizes sampled in this study ( $n \geq 13$ ) were in the range that can be described as “confined” rather than molecular.

Wang and co-workers reported a detailed determination of the structures of smaller  $\text{Na}_x\text{Cl}_{x+1}^-$  ( $x = 1-4$ ) clusters.<sup>205</sup> The clusters in this very small size range cannot assume any structure that resembles the cubic bulk structure, but they did feature connectivity with alternating Cl–Na–Cl atoms. An interesting feature of the clusters was that the excess negative charge was largely evenly shared between the halide atoms, with the electron binding energy increasing with  $x$ .

Bonding in metal oxide clusters can be described as a mixture of ionic and covalent bonding. Metal oxide clusters offer a platform for determining the evolution of cluster properties with sequential oxidation, as illustrated in Fig. 1. Unsaturated, suboxide clusters offer an enticing atomic-scale view of the oxidation process, a non-smooth process because of their small size. The value addition of computational studies provides greater detail. For example, after the discovery of the first  $\text{Mn}_{12}$  single molecule magnet, Bowen and co-workers used a combination of anion PE spectroscopy and theory to explore the magnetic properties in small, profoundly reduced  $\text{Mn}_5\text{O}^-$  and  $\text{Mn}_6\text{O}^-$  clusters, revealing the existence of multiple

isomags, including non-magnetic species that would be undetected using other methods.<sup>206</sup>

While the electronic and molecular structures of small metal oxide clusters do reflect the bulk properties to a certain extent, particularly in fully oxidized clusters (e.g.,  $\text{Mo}_3\text{O}_9^-$  in Fig. 2), the combination of small size below which any proto-bulk structure is energetically favorable and lower-than-traditional oxidation states can lead to different structures favored for the anion and the neutral.<sup>207</sup> In such a case, the anion PE spectrum does not provide information on the adiabatic EA or structure of the lowest energy neutral structure. In the event of close-lying structures for both the anion and neutral, cluster anions tend to favor more extended structures or structures that can otherwise support a more delocalized charge distribution. In the case of  $\text{Al}_3\text{O}_3^-$ ,<sup>49</sup>  $\text{MoVO}_3^-$ ,<sup>199</sup> and several other clusters studied in our laboratory, at least two structural isomers of the anions were found to be computationally very close in energy and co-populated the ion beam, with one of the structures emerging definitively more favorable for the neutral.

An anion beam “hole-burning” strategy was adopted to partially deplete the anion with the lower binding energy (i.e., the structure associated with the more stable neutral) using a lower-photon energy laser prior to the ion packet entering the main laser interaction region. Figure 8 shows the spectra of (a)  $\text{Al}_3\text{O}_3^-$  and (b)  $\text{MoVO}_3^-$  obtained using 3.495 eV photon energy, both with and without the partial “bleaching” of one isomer, along with the deconvoluted spectra. Figure 8(c) shows how spectral features associated with the lower-energy neutral structure can be partially bleached if the anions are close in energy. Indeed, a series of studies on transition metal suboxide structures showed a relationship between the number M–O–M bridge bonds vs M = O terminal bonds and the electron binding energy, since neutrals favored the former, which make the cluster more compact, and anions favor the latter, which accommodates charge delocalization.

Anion PE spectra of lanthanide oxides have posed interesting challenges to the currently available low-cost electronic structure calculations.<sup>208–214</sup> With partially filled, core-like 4f subshells, a crush of close-lying electronic states with nearly identical orbital occupancies, and also with close-lying ferromagnetically and anti-ferromagnetically coupled states, their relative energies appear to be dependent on the charge state. Recently, we demonstrated that lanthanide suboxide clusters near the center of the row, such as Sm ( $4f^5$  or  $4f^6$ ) or Gd ( $4f^7$ ), exhibit the effects of strong photoelectron-valence electron (PEVE) interactions,<sup>215</sup> hallmarked by anti-Wigner threshold law behavior and the prevalence of shake-up transitions. Figure 9(a) shows one such example: the PE spectrum of  $\text{Sm}_2\text{O}^-$  measured using 3.495 eV photon energy exhibits an intense band X and two lower-intensity transitions or manifolds of transitions, A and B, at higher  $e^-BE$  (i.e., lower  $e^-KE$ ). With lower photon energy, the  $e^-KE$  values of all transitions drop and approach zero for A and B, yet the intensity of A (also less obviously, B) increases relative to band X. This behavior was rationalized as due to longer PEVE interaction times with lower  $e^-KE$ , leading more higher probabilities of mapping the perturbed [neutral +  $e^-$ ] system onto excited neutral final states, e.g., A and B.

The [neutral +  $e^-$ ] interaction time is on the fs timescale, regardless of the photon energy used in the detachment. However,

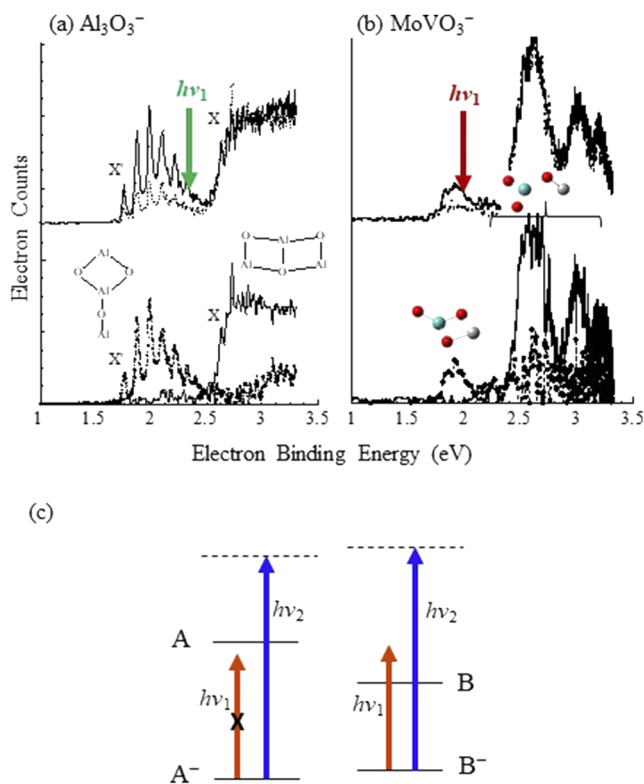


**FIG. 8.** Raw anion PE spectra of (a)  $\text{Al}_3\text{O}_3^-$  (Ref. 49) and (b)  $\text{MoVO}_3^-$  (Ref. 199) obtained using 3.495 eV photon energy (top, solid trace) and of the ion packets after the lower EA isomer was partially depleted with  $h\nu_1$  (2.330 eV for  $\text{Al}_3\text{O}_3^-$  and 2.016 eV for  $\text{MoVO}_3^-$ , dotted line at top). Bottom spectra show the deconvolution of the spectral contribution associated with the two different structural isomers for each. Turquoise represents Mo, gray represents V, and red represents O. (c) Schematic of relative energies of the anions and neutrals of isomers A and B in which isomer B is much lower in energy for the neutral. If  $A^-$  and  $B^-$  are close in energy, then  $B^-$  can be partially depleted by a  $h\nu_1$ , which does not detach  $A^-$  prior to the photoelectron spectrum being obtained using  $h\nu_2$ . (a) Adapted with permission from Akin and Jarrold, *J. Chem. Phys.* **118**, 1773 (2003). Copyright 2003 AIP Publishing LLC, and (b) Mann *et al.*, *J. Phys. Chem. A*, **114**, 11312 (2010). Copyright 2010 American Chemical Society.

electronic excitations are on the same timescale. Figure 9(b) shows one point of comparison: the electric field from the ejected electron felt by the neutral as a function of time for three different photon energies, assuming the momentum of the ejected electron remains constant, and a binding energy of  $\sim 1$  eV. An externally applied electric field is a time-dependent perturbation on the electronic structure of the neutral, particularly with highly polarizable outer valence orbitals. During the (evolving) perturbation, orbitals can be described as a time-dependent linear combination of the unperturbed orbitals, resulting in a wider range of final neutral states beyond the one-electron picture being accessed. In addition, fields on the order of  $0.4 \text{ V \AA}^{-1}$  are predicted to switch the relative stabilities of ferromagnetically coupled and antiferromagnetically coupled states.<sup>216</sup> The color-coded arrows in the bottom panel of Fig. 9 show the duration of fields over  $0.4 \text{ V \AA}^{-1}$  for three different photon energies. For systems in which the high density of low-lying states,

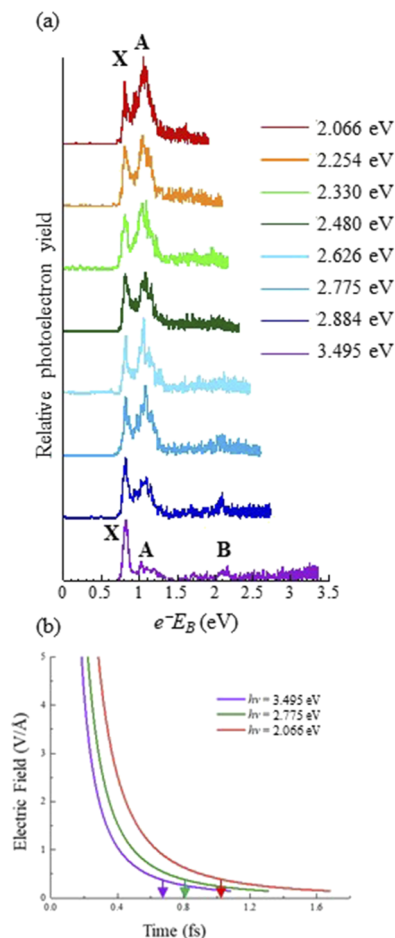


**FIG. 9.** (a) PE spectra of  $\text{Sm}_2\text{O}^-$  obtained over a range of photon energies (Ref. 215), showing the increase in the relative intensities of transitions to excited states with the decrease in photon energy and photoelectron  $e^-KE$ . The excited state populations increase with the increase in photoelectron–valence electron interaction time. (b) Field from the photoelectron as a function of time for transitions to excited states, driven by three photon energies. The color-coded arrows indicate the time at which the field is  $0.4 \text{ V \AA}^{-1}$ , which is sufficient to change the relative energies of FM and AFM states in computational studies (Ref. 216) on similar systems. (a) Reprinted with permission from Mason *et al.*, *J. Phys. Chem. Lett.* **10**, 144 (2019). Copyright 2019 American Chemical Society.

including close-lying ferromagnetic and antiferromagnetic states, create rich time-evolving [neutral +  $e^-$ ] interactions, the detachment process cannot be viewed as instantaneous, and transitions that would traditionally be described as shake-up or spin forbidden are apparently common.

Preceding was just a sampling of some of the interesting findings in mixed clusters, including purely ionic stoichiometric, incrementally non-stoichiometric, and several different types of metal oxides, ranging from profoundly reduced to stoichiometric. Beyond these classes of clusters studied by anion PE spectroscopy are metal sulfides,<sup>217,218</sup> mixed III–V, and II–VI cluster models for semiconductors and elemental combinations selected to model interfaces such as metal–semiconductor junctions or supported metal catalysts

at an atomic level. As an example, particularly stable metal–carbon clusters, or met-cars,<sup>219,220</sup> were discovered and explored in the gas phase, including via anion PE spectroscopy.<sup>221</sup> The met-cars possess alluring stoichiometries (e.g.,  $\text{Ti}_8\text{C}_{12}$ ) and high-symmetry structures, and appeared as magic numbers in mass spectra of ionic species. While these systems continue to be explored computationally as model catalysts, realization of their applications has proven elusive.

Mixed metal oxides, i.e., ternary clusters, add another dimension for exploring more complex electronic structures. Near-neighbor combinations such as the  $\text{MoVO}_y^-$ ,<sup>199</sup>  $\text{MoNbO}_y^-$ ,<sup>201</sup>  $\text{Mo}_x\text{W}_x'\text{O}_y^-$ ,<sup>196,203</sup>  $\text{Mn}_x\text{Mo}_x'\text{O}_y^-$ ,<sup>87</sup> and  $\text{Ce}_x\text{Sm}_x'\text{O}_y^-$ <sup>131,214</sup> studied in our group revealed that modest differences in metal oxophilicity can result in very pronounced differences in oxidation states of the individual metal centers for any suboxide species, which may underlie the particular activity of doped metal oxides in a reduced environment. Trans-periodic combinations, such as  $\text{AlMO}_y^-$  ( $M = \text{Mo}, \text{W}$ )<sup>200,202</sup> or  $\text{Ce}_x\text{O}_y\text{Pt}_n^-$ ,<sup>212</sup> are described as ionic complexes,  $\text{Al}^+[\text{MO}_y]^{2-}$  and  $[\text{Ce}_x\text{O}_y]^+\text{Pt}_n^{2-}$ , which have implications for supported metal and metal oxide catalysts, and the electrostatic environment at the interface between the catalyst and support material. While cluster models of catalysts have obvious limitations in accounting for all the chemical and physical features at play in applied systems, they do provide important insight into important atomic and molecular scale features that govern catalyst–substrate interactions.

### C. “Doped” clusters

As a variation on the theme of mixed-elemental clusters, doped clusters can be distinguished as being prevalently one element (or one compound, such as a monometallic oxide) to which a disparate atom is added. Doped clusters have a rich history in cluster studies. The notion and appeal of clusters that are air stable were in full flower following the discovery of  $\text{C}_{60}$  and were further fueled by the production of air-stable single-metal atom encapsulated fullerenes.<sup>222</sup> Endohedrally doped cage clusters, an idea built on fullerene encapsulated metals,<sup>223</sup> have continued to be actively explored. These high-symmetry species, and understanding their growth, have motivated the study of smaller metal-doped group IV clusters using anion PE spectroscopy,<sup>224–227</sup> which, when combined with computational studies, show the evolution in electronic and structural properties as the clusters grow toward the more symmetric and stable cage-like structures. Nuanced information such as charge distribution between the dopant and the main cluster can also be gleaned from calculations, provided some reconciliation between the calculated structures and observed spectra.<sup>228</sup> These studies show that within the small ( $n < 20$ ) cluster size regime, a single dopant atom can have a profound effect on the cluster structure and stability.

In a similar vein to magic number met-cars and other metal-doped group IV clusters, the concept of “designer magnetic superatoms” has been explored by Zhang *et al.*<sup>229</sup> They proposed that simple elemental superatomic clusters doped with a single magnetic atom, e.g.,  $\text{VNa}_7$ , would provide stability with a high magnetic moment. Rather than relying on the traditional approach of a Stern–Gerlach setup to measure the magnetic moments of the V-doped Na clusters, they relied on comparing experimental and

computational spectra, with the calculations on structures and spin states in agreement with the observed spectra providing the magnetic moment.

In an elegant extension of their work on elemental boron clusters, Wang and co-workers have conducted a series of studies on doped boron clusters,  $\text{MB}_n^-$ ,<sup>123,230–232</sup> with dopants ranging from Li to transition metals to lanthanides. The strength of B–B bonding results in structures that could aptly be described as  $\text{B}_x^-$  cluster-ligated metal centers. For example, the high-spin metalboron cluster,  $\text{MnB}_6^-$ , studied with high resolution PEI spectroscopy was shown to have a planar teardrop structure with Mn at its “tip”<sup>233</sup> and a stable aromatic electronic structure. Other transition metal doped boron clusters assume beautiful flower-like structures, with the metal center as the pistil and the ring- or drum-like boron clusters structure encircling the metal center, as shown in Fig. 10.<sup>230</sup>

Lanthanide hexaborides are cluster materials used in electron emitters and have exotic magnetic properties. In the bulk,  $\text{B}_6$  octahedral anions form a cubic lattice with the lanthanide cations, but in small clusters, the negatively charged  $\text{B}_6$  unit is planar or near-planar. Bowen and co-workers<sup>234</sup> and our group<sup>131</sup> have probed  $\text{SmB}_6^-$  and  $\text{CeB}_6^-$ , respectively, where both have the lowest energy structures evocative of a teardrop with the metal center at the tip.  $\text{CeB}_6$  was determined to be highly ionic, with  $\text{Ce}^{2+}(\text{B}_6)^{3-}$  aptly describing the anion, while the spectrum of  $\text{SmB}_6^-$  coupled with *ab initio* calculations suggested some covalent character involving the 4f orbitals of Sm overlapping with  $\text{B}_6$ -local orbitals. Wang and co-workers recently reported a bent triple-decker inverse-sandwich structure of  $\text{La}_3\text{B}_{14}^-$ , which gives hints of the more compact boride cluster structures found in the bulk material.<sup>235</sup>

### D. Ligated clusters

As noted in the Introduction, a large body of metal and metal oxide cluster studies implement clusters as models for catalysts. A particularly useful feature of cluster models is the ability to emulate defect sites in a controlled, albeit somewhat reductionist, manner. However, there have been numerous experimental studies, outside of anion PE spectroscopy, on metal and metal oxide clusters ligated with  $\text{CO}_2$ ,  $\text{CO}$ ,  $\text{H}_2$ , ethylene, and other molecules that have shed

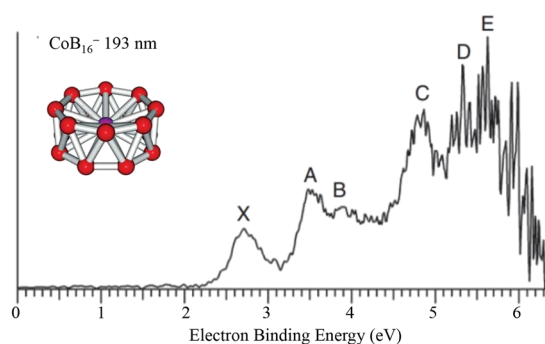


**FIG. 10.** PE spectrum and structure of the Co-doped  $\text{B}_{16}^-$  cluster (Ref. 230). Popov *et al.*, Nat. Commun. **6**, 8654 (2015). Copyright 2015 licensed under a Creative Commons Attribution (CC BY 4.0) license. The authors edited the figures from Ref. 230 by superimposing the molecular structure on the spectrum.

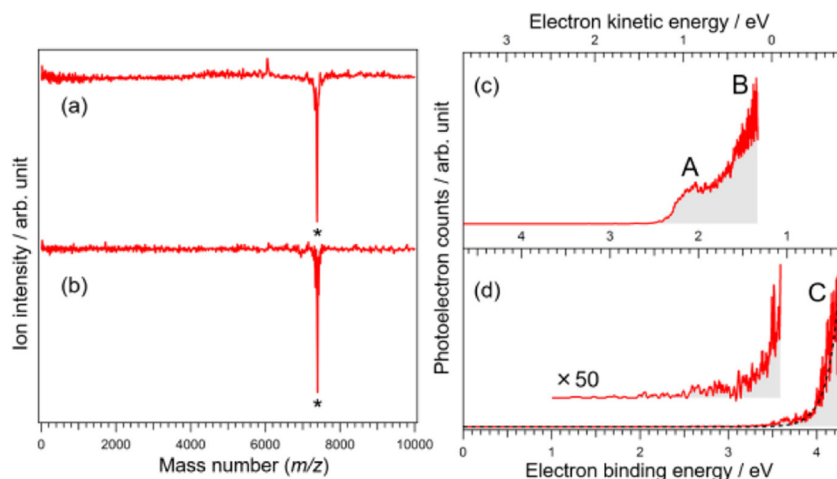


**FIG. 11.** From Ref. 250: photodetachment difference mass spectra of  $[\text{Au}_{25}(\text{SC}_2\text{H}_4\text{Ph})_{18}]^-$  at (a) 355 nm and (b) 266 nm. The asterisks point to the depletion of parent ions. PE spectra of  $[\text{Au}_{25}(\text{SC}_2\text{H}_4\text{Ph})_{18}]^-$  at (c) 355 nm and (d) 266 nm. Red solid and black dotted lines correspond to the experimental data and simulated curves for thermionic emission from the  $\text{Au}_{13}$  core, respectively. Reprinted with permission from Hirata *et al.*, *J. Phys. Chem. C* **123**, 13174 (2019). Copyright 2019 American Chemical Society.

light on the interactions between catalytically active sites and substrates. One of the more effective experimental tools in this arena has proven to be IR predissociation spectra of ions.<sup>15,22–25,77,78</sup> The added value of anion photodetachment studies on cluster complexes with molecules such as  $\text{H}_2$ ,<sup>236</sup>  $\text{CO}$ ,<sup>237–240</sup>  $\text{C}_2\text{H}_2$ ,<sup>241</sup> and  $\text{CO}_2$  and larger molecules such as amines<sup>242</sup> and benzene<sup>243</sup> is a direct insight into how the charge state impacts the cluster–ligand interactions. For example, in metal cluster carbonyl complexes, the excess charge on the anion leads to enhanced  $\pi^*$  back-donation, and detachment spectra exhibit progressions in the C–O stretch, resulting from preparing the neutral cluster complex with elongated carbonyl bonds.<sup>244</sup> Studies on smaller, ligated heterometallic clusters can give insight into the nature of doping sites or cooperative catalyst.<sup>245,246</sup>

More recent studies on ligated clusters leverage advances in coupling ESI sources and cryogenic ion traps to pulsed anion photoelectron spectrometers,<sup>247</sup> which have facilitated studies on solution-phase synthesized ligated clusters. As anionic ligated clusters can also shed ligands while being introduced into the gas phase by ESI, probing the progression, or tuning, of properties of the bare clusters to saturated, ligated clusters in the absence of solvent molecules is achieved. An illustration of this effect can be found in work of Bowen and co-workers on ligated cobalt sulfide clusters.<sup>248,249</sup> By sequentially ligating the superatomic  $\text{Co}_6\text{S}_8$  cluster with electron-donating triethyl phosphine ligands, which form dative bonds with the metal centers, they demonstrated a sequential decrease in EA of the neutral.<sup>248</sup> Furthermore, sequential substitution of CO ligands for the triethyl phosphine ligands, i.e.,  $\text{Co}_6\text{S}_8(\text{PEt}_3)_{6-x}(\text{CO})_x$  ( $x = 0–3$ ), resulted in a systematic increase in EA. Additional insight from the computational component of this study included the demagnetization of the  $\text{Co}_6\text{S}_8$  core with ligation.

An example of anion PE studies on ligated gold and silver clusters synthesized via benchtop methods for making molecularly homogeneous species is the work by Hirata *et al.*, who introduced  $[\text{Au}_{25}(\text{SR})_{18}]^-$  and  $[\text{Ag}_{25}(\text{SR})_{18}]^-$  thiolate complexes into a magnetic bottle instrument.<sup>250</sup> In the case of these ligated metallic species, photodissociation through loss of thiolate (anionic) ligands competes with photodetachment, as shown in Figs. 11(a) and 11(b). Direct detachment spectra were observed with 3.495 eV photon

energy [Fig. 11(c)], with the spectrum exhibiting two broad transitions, allowing a determination of the EA. However, with 4.661 eV photon energy, thermionic emission was observed exclusively, suggesting a large oscillator strength direct absorption transition completely usurping any direct detachment. These findings underscore the need to take into account indirect processes as a matter of course for more complex systems, and indeed, direct detachment may not be observed in studies on certain anions.

#### IV. OUTLOOK

Anion PE spectroscopies on the wide array of “hard” clusters have brought a wealth of insight into the evolution of properties with size and composition. With advances in the techniques for generating, mass-selecting, and probing cluster anions using different flavors of anion detachment, it has become evident that additional, exciting information can be gleaned from these types of studies.

##### A. Mining additional information embedded in anion PE spectra

As described in Sec. III D, the anion PE spectra of  $[\text{Au}_{25}(\text{SR})_{18}]^-$  and  $[\text{Ag}_{25}(\text{SR})_{18}]^-$  clusters exhibited primarily thermionic emission, rather than detachment, under ultraviolet radiation. At some size or cluster composition, does anion photodetachment no longer provide useful information? Can more be gleaned from indirect processes? Given that this effect was clearly photon energy-dependent, measuring PE spectra over a range of photon energies and plotting the ratio of direct detachment to thermionic emission signal could provide the gas phase electronic absorption spectrum of the anions while concurrently mapping the neutral electronic structures. If mass analysis is conducted in parallel, photodissociation vs photoexcitation/thermionic emission pathways can be explored, which would provide more insight into the nature of the excitations.

Similarly, more can be gleaned from anion PE spectra of clusters with exceptionally complex electronic structures, such as the lanthanide suboxide species, with a more rigorous theoretical treatment of the detachment process. Computational results are essential to a large body of cluster study, yet the photodetachment process is

not fully understood. Detachment transitions have generally been treated as “sudden” or “instantaneous,” while more recent experimental studies on strongly correlated systems demonstrate that they are not and that strong photoelectron–valence electron interactions can add a dimension to the analysis of the detachment spectra, including mapping the energies and character of excited states that are dark with respect to direct detachment. Additional detailed information on the multi-stable magnetic states and the effects of the time-dependent inhomogeneous electric field generated by the photoelectron, or other interesting phenomena such as the multiferroic states of  $Rh_n$  clusters,<sup>251</sup> can be better understood with more detailed theoretical support. Furthermore, a more rigorous treatment of the time-dependent nature of detachment transitions would deeply enrich our understanding of increasingly complex systems, including a number of large non-cluster systems (e.g., extended conjugated biological molecules) with high densities of states, and electron–neutral interactions involved in electron-driven chemistry more generally.

## B. Dynamics of the electronic states of neutral clusters

With the ever-improving spectroscopic “shutter speed,” the ultrafast dynamics of electronic excitation and relaxation can be probed. The work by Neumark on  $Hg_n$  anions<sup>119,120</sup> reveals the range of size-dependent relaxation processes associated with the protoband structure of small semiconductor clusters; unusually fast relaxation times coupled with nuclear wave packet motion with excitation were also observed. In principle, these types of measurements can be extended to neutral clusters. Most of the anion photodetachment spectra of clusters described in this perspective exhibit transitions to excited neutral states (including multi-electron transitions), the temporal evolution of which can further be explored either by a second ionizing pulse or through sensitive fluorescence measurements. These measurements will be complicated if there are multiple excited states accessed in the detachment and further complicated with vibrationally broadened transitions. However, the fact that different spin states are accessed via anion detachment will create an interesting landscape, wherein spin-allowed vs spin-forbidden relaxations can be inferred. Exploration into the use of x-ray free electron lasers (XFELs) as a route for core-level photoelectron spectroscopy and ultrafast dynamics of size-selected anionic clusters is also currently under way.<sup>252</sup> Although challenging, these studies offer promising insight into the relaxation dynamics of the neutral cluster and photoelectron–neutral interactions.

In the case of time-resolved detachment-ionization measurements, ionization energies of cluster are generally significantly higher than their associated electron affinities, although certain classes of clusters, most notably, alkali, lanthanide, and lanthanide suboxide clusters, have very low ionization energies,  $\sim 4$  eV,<sup>253</sup> so ionizing excited states of the neutral clusters would be in the visible to ultraviolet range. Using the lanthanide oxide clusters with the spectra exhibiting shake-up (multi-electron) transitions to excited states, the fates of these states can be followed by mapping the total cation yield as a function of delay time. Furthermore, the detachment energy has been shown to change the relative abundances of excited states. Measuring the  $e^- KE$  of the whole system, which will

include detachment and ionization transitions, as a function of the detachment energy will provide a tidy tie line through anion detachment spectroscopies and PFI-ZEKE measurements while providing dynamical information on intermediate neutral states.

## C. Stepping toward more realistic models for catalysts

The prospect of building new bulk catalytic materials from cluster deposition underscores the overall importance of cluster studies while simultaneously motivating the development of instrumentation for cluster species selectivity. An important question is how do the electronic properties of isolated clusters change upon deposition? Anderson and co-workers have devoted significant effort into studying the size-selected deposition of metal atoms onto surfaces of support materials such as  $TiO_2$ .<sup>254,255</sup> When deposited on a surface, the catalytic properties of metal clusters have unique, discrete energy levels from the respective individual atoms, gas phase clusters, and bulk material. Howard-Fabretto and Andersson discussed this phenomenon in a recent review, which focuses primarily on the photocatalytic properties of Au and Ru clusters deposited on semiconductor surfaces.<sup>256</sup> Current cluster beam methods are capable of building bulk catalytic materials in a laboratory setting, but preparative scale cluster deposition techniques are still needed.<sup>257</sup> Ideally, the integrity (or enhancement) of the clusters' catalytic activity is maintained by deposition onto a weakly interacting substrate, such as highly ordered graphite,<sup>258</sup> which also motivates further study leading toward developing predictability of the properties of clusters measured in the gas phase, after deposition on surfaces.

Cluster models also are useful in shedding light on defect sites in bulk material. These sites often present in the form of edge sites, basal planes, and vacancies and sometimes contribute significantly to the overall catalytic activity of the material. In regard to the oxygen reduction reaction (ORR) and hydrogen evolution reaction (HER), these defect sites are widely considered to be the most active catalytic sites in the material due to their tuned electronic properties.<sup>19–22</sup> Studies for the past two decades have focused on tuning the electronic properties of these sites by doping. Since these sites are localized, clusters studies are commonly utilized to gain information on catalytic behaviors of these materials. For example, metal sulfides have localized bonding and defect sites, making cluster models an excellent representation of molecular catalytic processes.<sup>23</sup> In addition, graphene point and line defects have been shown to have ORR electrocatalytic capability with energy barriers comparable to platinum(111).<sup>20</sup> These cluster studies have a primary interest in understanding molecular reaction pathways that lead to kinetic macroscopic properties of the material.

## D. Underexplored techniques and questions

The more common application of cryogenic traps coupled to cluster sources in the past decade has allowed us to look at internally cold systems, which decongest spectra by suppressing hot bands and rotational broadening, allowing for more definitive and simplified analyses. Clusters generally do not reach the temperature of the cryogenic trap, however. Helium nanodroplets, on the other hand, are an ultracold vehicle for spectroscopic measurements. Metal clusters

have been synthesized in He droplets,<sup>259</sup> and neutral photoionization spectra of Mg clusters in He nanodroplets have been measured,<sup>260</sup> offering the tantalizing possibility of anion PE spectroscopy of ultracold clusters in He nanodroplets. One potential pitfall would be broadening by He “boiling” off the neutral cluster due to the large change in cluster–He interaction with the charge state.

In a reversal of using photodetachment to probe strong photoelectron-valence electron interactions near detachment threshold, strong electron–neutral interactions in certain systems may lead to interesting electron attachment processes. Using older electron transmission spectroscopy techniques on these more exotic species, the anions of which can be  $m/z$  selected and photodetached prior to interrogation by a monochromatic electron, unbound anionic states that are strongly coupled to bound states can be explored. Such studies may yield more insight into “doorway” states for anion formation and electron momentum control of anion or neutral state populations.

Certainly, the range of cluster systems studied by anion photodetachment can continue to augment our understanding of the evolution of the band structure from the atomic or molecular scale to the bulk, the nature of defect sites in catalysts, the catalytic activities of small clusters of inert bulk, and strong electron neutral interactions. Beyond these areas that have already been visited to varying degrees, entanglement, quantum information, single molecule magnets, and spintronics offer areas into which anion PE spectroscopy studies of small clusters could continue to expand and flourish.

## ACKNOWLEDGMENTS

C.C.J. is grateful for enlightening conversations with Professor Hrant P. Hratchian (UC Merced) and for additional graphics from Professor K.H. Bowen (JHU), Professor L.-S. Wang (Brown), and Professor G.B. Ellison (CU Boulder). This work was supported by the Indiana University College of Arts and Sciences.

## DATA AVAILABILITY

Data sharing is not applicable to this article as no new data were created or analyzed in this study.

## REFERENCES

- 1 A. P. Kaldor, D. M. Cox, and M. R. Zakin, “Molecular surfaces: Chemistry and physics of gas phase clusters,” in *Microclusters*, Springer Series in Materials Science, Vol. 4, edited by S. Sugano, Y. Nishina, and S. Ohnishi (Springer, Berlin, Heidelberg, 1987).
- 2 M. Moskovits and J. E. Hulse, *J. Chem. Soc., Faraday Trans. 2* **73**, 471 (1977).
- 3 H. Haberland, *Clusters of Atoms and Molecules*, Springer Series in Chemical Physics, Vol. 52 (Springer, Berlin, 1994).
- 4 M. D. Morse, “Clusters of transition-metal atoms,” *Chem. Rev.* **86**, 1049 (1986).
- 5 *Metal Clusters*, edited by W. Ekardt (Wiley, New York, 1999).
- 6 *Advances in Metal and Semiconductor Clusters*, edited by M. A. Duncan (Elsevier, 2001), Vol 1-5.
- 7 W. A. de Heer, *Rev. Mod. Phys.* **65**, 611 (1993).
- 8 D. C. Parent and S. L. Anderson, *Chem. Rev.* **92**, 1541 (1992).
- 9 A. W. Castleman and K. H. Bowen, *J. Phys. Chem.* **100**, 12911 (1996).
- 10 C. T. Wolke, J. A. Fournier, L. C. Dzigan, M. R. Fagiani, T. T. Odbadrakh, H. Knorke, K. D. Jordan, A. B. McCoy, K. R. Asmis, and M. A. Johnson, *Science* **354**, 1131 (2016).
- 11 R. M. Young and D. M. Neumark, *Chem. Rev.* **112**, 5553 (2012).
- 12 T. I. Yacovitch, T. Wende, L. Jiang, N. Heine, G. Meijer, D. M. Neumark, and K. R. Asmis, *J. Phys. Chem. Lett.* **2**, 2135 (2011).
- 13 K. R. Leopold, *Annu. Rev. Phys. Chem.* **62**, 327 (2011).
- 14 A. Fujii and K. Mizuse, *Int. Rev. Phys. Chem.* **32**, 266 (2013).
- 15 N. Heine and K. R. Asmis, *Int. Rev. Phys. Chem.* **34**, 1 (2015).
- 16 W. T. S. Cole and R. J. Saykally, *J. Chem. Phys.* **147**, 064301 (2017).
- 17 Z. Bačić and R. E. Miller, *J. Phys. Chem.* **100**, 12945 (1996).
- 18 S. M. Lang, T. M. Bernhardt, J. M. Bakker, B. Yoon, and U. Landman, *Int. J. Mass Spectrom.* **435**, 241 (2019).
- 19 D. K. Böhme and H. Schwarz, *Angew. Chem., Int. Ed.* **44**, 2336 (2005).
- 20 N. Dietl, X. Zhang, C. van der Linde, M. K. Beyer, M. Schlangen, and H. Schwarz, *Chem. Eur. J.* **19**, 3017 (2013).
- 21 E. Barwa, T. F. Pascher, M. Ončák, C. Linde, and M. K. Beyer, *Angew. Chem., Int. Ed.* **59**, 7467 (2020).
- 22 L. G. Dodson, M. C. Thompson, and J. M. Weber, *J. Phys. Chem. A* **122**, 6909 (2018).
- 23 L. G. Dodson, M. C. Thompson, and J. M. Weber, *J. Phys. Chem. A* **122**, 2983 (2018).
- 24 J. H. Marks, T. B. Ward, and M. A. Duncan, *Int. J. Mass Spectrom.* **435**, 107 (2019).
- 25 T. B. Ward, A. D. Brathwaite, and M. A. Duncan, *Top. Catal.* **61**, 49 (2018).
- 26 A. E. Green, S. Schaller, G. Meizyte, B. J. Rhodes, S. P. Kealy, A. S. Gentleman, W. Schöllkopf, A. Fielicke, and S. R. Mackenzie, *J. Phys. Chem. A* **124**, 5389 (2020).
- 27 G. Meizyte, A. E. Green, A. S. Gentleman, S. Schaller, W. Schöllkopf, A. Fielicke, and S. R. Mackenzie, *Phys. Chem. Chem. Phys.* **22**, 18606 (2020).
- 28 M. P. Klein, A. A. Ehrhard, J. Mohrbach, S. Dillinger, and G. Niedner-Schatteburg, *Top. Catal.* **61**, 106 (2018).
- 29 S. Dillinger, J. Mohrbach, and G. Niedner-Schatteburg, *J. Chem. Phys.* **147**, 184305 (2017).
- 30 S. Debnath, X. Song, M. R. Fagiani, M. L. Weichman, M. Gao, S. Maeda, T. Taketsugu, W. Schöllkopf, A. Lyalin, D. M. Neumark, and K. R. Asmis, *J. Phys. Chem. C* **123**, 8439 (2019).
- 31 S. Yin, Z. Wang, and E. R. Bernstein, *J. Chem. Phys.* **139**, 084307 (2013).
- 32 G. E. Johnson, R. Mitrić, M. Nössler, E. C. Tyo, V. Bonačić-Koutecký, and A. W. Castleman, Jr., *J. Am. Chem. Soc.* **131**, 5460 (2009).
- 33 D. J. Xiao, E. D. Bloch, J. A. Mason, W. L. Queen, M. R. Hudson, N. Planas, J. Borycz, A. L. Dzubak, P. Verma, K. Lee, F. Bonino, V. Crocellà, J. Yano, S. Bordiga, D. G. Truhlar, L. Gagliardi, C. M. Brown, and J. R. Long, *Nat. Chem.* **6**, 590 (2014).
- 34 E. F. Fialko, A. V. Kikhtenko, V. B. Goncharov, and K. I. Zamaraev, *J. Phys. Chem. A* **101**, 8607 (1997).
- 35 Z.-C. Wang, S. Yin, and E. R. Bernstein, *J. Phys. Chem. A* **117**, 2294 (2013).
- 36 W. Xue, Z.-C. Wang, S.-G. He, Y. Xie, and E. R. Bernstein, *J. Am. Chem. Soc.* **130**, 15879 (2008).
- 37 D. R. Justes, R. Mitrić, N. A. Moore, V. Bonačić-Koutecký, and A. W. Castleman, Jr., *J. Am. Chem. Soc.* **125**, 6289 (2003).
- 38 A. W. Castleman, Jr., *Catal. Lett.* **141**, 1243 (2011).
- 39 B. V. Reddy, F. Rasouli, M. R. Hajaligol, and S. N. Khanna, *Chem. Phys. Lett.* **384**, 242 (2004).
- 40 B. V. Reddy and S. N. Khanna, *Phys. Rev. Lett.* **93**, 068301 (2004).
- 41 Y.-X. Zhao, X.-L. Ding, Y.-P. Ma, Z.-C. Wang, and S.-G. He, *Theor. Chem. Acc.* **127**, 449 (2010).
- 42 M. M. Kappes and R. H. Staley, *J. Am. Chem. Soc.* **103**, 1286 (1981).
- 43 Z. Li, Z. Fang, M. S. Kelley, B. D. Kay, R. Rousseau, Z. Dohnalek, and D. A. Dixon, *J. Phys. Chem. C* **118**, 4869 (2014).
- 44 Z.-C. Wang, X.-N. Wu, Y.-X. Zhao, J.-B. Ma, X.-L. Ding, and S.-G. He, *Chem. Eur. J.* **17**, 3449 (2011).
- 45 C. J. Mundy, J. Hutter, and M. Parrinello, *J. Am. Chem. Soc.* **122**, 4837 (2000).
- 46 U. Buck and C. Steinbach, *J. Phys. Chem. A* **102**, 7333 (1998).
- 47 L. Bewig, U. Buck, S. Rakowsky, M. Reymann, and C. Steinbach, *J. Chem. Phys. A* **102**, 1124 (1998).
- 48 F. A. Akin and C. C. Jarrold, *J. Chem. Phys.* **120**, 8698 (2004).
- 49 F. A. Akin and C. C. Jarrold, *J. Chem. Phys.* **118**, 1773 (2003).

- <sup>50</sup>U. Das, K. Raghavachari, and C. C. Jarrold, *J. Chem. Phys.* **122**, 014313 (2005).
- <sup>51</sup>D. M. Cox, D. J. Trevor, R. L. Whetten, and A. Kaldor, *J. Phys. Chem.* **92**, 421 (1988).
- <sup>52</sup>A. C. Reber, S. N. Khanna, P. J. Roach, W. H. Woodward, and A. W. Castleman, *J. Phys. Chem. A* **114**, 6071 (2010).
- <sup>53</sup>H.-G. Xu, X.-N. Li, X.-Y. Kong, S.-G. He, and W.-J. Zheng, *Phys. Chem. Chem. Phys.* **15**, 17126 (2013).
- <sup>54</sup>G. K. Koyanagi, D. K. Bohme, I. Kretzschmar, D. Schröder, and H. Schwarz, *J. Phys. Chem. A* **105**, 4259 (2001).
- <sup>55</sup>J.-B. Ma, Y.-X. Zhao, S.-G. He, and X.-L. Ding, *J. Phys. Chem. A* **116**, 2049 (2012).
- <sup>56</sup>S. Feyel, D. Schröder, and H. Schwarz, *Eur. J. Inorg. Chem.* **2008**, 4961.
- <sup>57</sup>F. Aubriet, J.-J. Gaumet, W. A. de Jong, G. S. Groenewold, A. K. Gianotto, M. E. McIlwain, M. J. van Stipdonk, and C. M. Leavitt, *J. Phys. Chem. A* **113**, 6239 (2009).
- <sup>58</sup>E. K. Parks, B. H. Weiller, P. S. Bechthold, W. F. Hoffman, G. C. Nieman, L. G. Pobo, and S. J. Riley, *J. Chem. Phys.* **88**, 1622 (1988).
- <sup>59</sup>H. Wei, X. Liu, A. Wang, L. Zhang, B. Qiao, X. Yang, Y. Huang, S. Miao, J. Liu, and T. Zhang, *Nat. Commun.* **5**, 5634 (2014).
- <sup>60</sup>J. M. Thomas, *Nature* **525**, 325 (2015).
- <sup>61</sup>G. Vilé, D. Albani, M. Nachttegaal, Z. Chen, D. Dontsova, M. Antonietti, N. López, and J. Pérez-Ramírez, *Angew. Chem., Int. Ed.* **54**, 11265 (2015).
- <sup>62</sup>M. Yang, J. Liu, S. Lee, B. Zugic, J. Huang, L. F. Allard, and M. Flytzani-Stephanopoulos, *J. Am. Chem. Soc.* **137**, 3470 (2015).
- <sup>63</sup>L.-N. Wang, X.-N. Li, L.-X. Jiang, B. Yang, Q.-Y. Liu, H.-G. Xu, W.-J. Zheng, and S.-G. He, *Angew. Chem., Int. Ed.* **57**, 3349 (2018).
- <sup>64</sup>A. B. Wolk, C. M. Leavitt, J. A. Fournier, M. Z. Kamrath, G. B. Wijeratne, T. A. Jackson, and M. A. Johnson, *Int. J. Mass Spectrom.* **354-355**, 33 (2013).
- <sup>65</sup>K. R. Asmis, *Phys. Chem. Chem. Phys.* **14**, 9270 (2012).
- <sup>66</sup>O. Hübner and H. J. Himmelf, *Chem. -A Eur. J.* **24**, 8941 (2018).
- <sup>67</sup>Y. Gong, M. Zhou, and L. Andrews, *Chem. Rev.* **109**, 6765 (2009).
- <sup>68</sup>I. M. L. Billas, A. Châtelain, and W. A. de Heer, *Surf. Rev. Lett.* **03**, 429 (1996).
- <sup>69</sup>Z. Luo and S. N. Khanna, *Metal Clusters and Their Reactivity* (Springer, Singapore, 2020).
- <sup>70</sup>Z. Luo, A. W. Castleman, Jr., and S. N. Khanna, *Chem. Rev.* **116**, 14456 (2016).
- <sup>71</sup>J. Berkowitz, *Photoabsorption, Photoionization, and Photoelectron Spectroscopy* (Academic, New York, 1979).
- <sup>72</sup>H.-J. Zhai, X. Huang, T. Waters, X.-B. Wang, R. A. J. O'Hair, A. G. Wedd, and L.-S. Wang, *J. Phys. Chem. A* **109**, 10512 (2005).
- <sup>73</sup>X. Huang, H.-J. Zhai, J. Li, and L.-S. Wang, *J. Phys. Chem. A* **110**, 85 (2006).
- <sup>74</sup>M. F. Jarrold and J. E. Bower, *J. Phys. Chem.* **92**, 5702 (1988).
- <sup>75</sup>M. Beyer, C. Berg, S. Joos, U. Achatz, W. Heringer, G. Niedner-Schatteburg, and V. E. Bondybey, *Int. J. Mass Spectrom.* **185-187**, 625-638 (1999).
- <sup>76</sup>A. Aguado and M. F. Jarrold, *Annu. Rev. Phys. Chem.* **62**, 151 (2011).
- <sup>77</sup>C. W. Copeland, M. A. Ashraf, E. M. Boyle, and R. B. Metz, *J. Phys. Chem. A* **121**, 2132 (2017).
- <sup>78</sup>M. D. Johnston, S. P. Lockwood, and R. B. Metz, *J. Chem. Phys.* **148**, 214308 (2018).
- <sup>79</sup>D. G. Leopold, J. Ho, and W. C. Lineberger, *J. Chem. Phys.* **86**, 1715 (1987).
- <sup>80</sup>J. Ho, K. M. Ervin, and W. C. Lineberger, *J. Chem. Phys.* **93**, 6987 (1990).
- <sup>81</sup>G. Ganteför, H. R. Siekmann, H. O. Lutz, and K. H. Meiwes-Broer, *Chem. Phys. Lett.* **165**, 293 (1990).
- <sup>82</sup>H. R. Siekmann, C. Lüder, J. Faehrmann, H. O. Lutz, and K. H. Meiwes-Broer, *Z. Phys. D: At., Mol. Clusters* **20**, 417 (1991).
- <sup>83</sup>T. G. Dietz, M. A. Duncan, D. E. Powers, and R. E. Smalley, *J. Chem. Phys.* **74**, 6511 (1981).
- <sup>84</sup>V. E. Bondybey and J. H. English, *J. Chem. Phys.* **74**, 6978 (1981).
- <sup>85</sup>R. L. Wagner, W. D. Vann, and A. W. Castleman, *Rev. Sci. Instrum.* **68**, 3010 (1997).
- <sup>86</sup>A. Nakajima, T. Kishi, T. Sugioka, Y. Sone, and K. Kaya, *J. Phys. Chem.* **95**, 6833 (1991).
- <sup>87</sup>J. L. Mason, A. K. Gupta, A. J. McMahon, C. N. Folluo, K. Raghavachari, and C. C. Jarrold, *J. Chem. Phys.* **152**, 054301 (2020).
- <sup>88</sup>C. M. Neal, G. A. Breaux, B. Cao, A. K. Starace, and M. F. Jarrold, *Rev. Sci. Instrum.* **78**, 075108 (2007).
- <sup>89</sup>S. E. Waller, J. E. Mann, and C. C. Jarrold, *J. Phys. Chem. A* **117**, 1765 (2013).
- <sup>90</sup>W. Bouwen, P. Thoen, F. Vanhoutte, S. Bouckaert, F. Despa, H. Weidele, R. E. Silverans, and P. Lievens, *Rev. Sci. Instrum.* **71**, 54 (2000).
- <sup>91</sup>N. X. Truong, M. Haertelt, B. K. A. Jaeger, S. Gewinner, W. Schöllkopf, A. Fielicke, and O. Dopfer, *Int. J. Mass Spectrom.* **395**, 1 (2016).
- <sup>92</sup>M. Oujja, J. G. Izquierdo, L. Bañares, R. De Nalda, and M. Castillejo, *Phys. Chem. Chem. Phys.* **20**, 16956 (2018).
- <sup>93</sup>M. Oujja, M. Sanz, A. Martínez-Hernández, I. López-Quintas, J. G. Izquierdo, L. Bañares, and M. Castillejo, in *13th European Conference on Atoms Molecules and Photons*, edited by (European Physical Society, 2019).
- <sup>94</sup>J. Perrière, C. Boulmer-Leborgne, R. Benzerga, and S. Tricot, *J. Phys. D: Appl. Phys.* **40**, 7069 (2007).
- <sup>95</sup>G. Liu, S. M. Ciborowski, and K. H. Bowen, *J. Phys. Chem. A* **121**, 5817 (2017).
- <sup>96</sup>L.-S. Wang, *J. Chem. Phys.* **143**, 040901 (2015).
- <sup>97</sup>K. H. Bowen and J. G. Eaton, in *The Structure of Small Molecules and Ions*, edited by R. Naaman and Z. Vager (Plenum, New York, 1988), pp. 147-169.
- <sup>98</sup>J. Cooper and R. N. Zare, *J. Chem. Phys.* **48**, 942 (1968).
- <sup>99</sup>A. Sanov, *Annu. Rev. Phys. Chem.* **65**, 341 (2014).
- <sup>100</sup>M. J. Travers, D. C. Cowles, E. P. Clifford, G. B. Ellison, and P. C. Engelking, *J. Chem. Phys.* **111**, 5349 (1999).
- <sup>101</sup>C. Bordas, F. Paulig, H. Helm, and D. L. Huestis, *Rev. Sci. Instrum.* **67**, 2257 (1996).
- <sup>102</sup>C. Strobel, G. Ganteför, A. Bodi, and P. Hemberger, *J. Electron Spectrosc. Relat. Phenom.* **239**, 146900 (2020).
- <sup>103</sup>M. Vonderach, O. T. Ehrler, P. Weis, and M. M. Kappes, *Anal. Chem.* **83**, 1108 (2011).
- <sup>104</sup>A. Sanov and R. Mabbs, *Int. Rev. Phys. Chem.* **27**, 53-85 (2008).
- <sup>105</sup>A. T. J. B. Eppink and D. H. Parker, *Rev. Sci. Instrum.* **68**, 3477 (1997).
- <sup>106</sup>M. Van Duzor, F. Mbaiwa, J. Lasinski, N. Holtgrewe, and R. Mabbs, *J. Chem. Phys.* **134**, 214301 (2011).
- <sup>107</sup>J. Lyle, T.-C. Jagau, and R. Mabbs, *Faraday Discuss.* **217**, 533 (2019).
- <sup>108</sup>B. A. Laws, S. J. Cavanagh, B. R. Lewis, and S. T. Gibson, *J. Phys. Chem. A* **123**, 10418 (2019).
- <sup>109</sup>B. A. Laws, S. J. Cavanagh, B. R. Lewis, and S. T. Gibson, *J. Phys. Chem. Lett.* **8**, 4397 (2017).
- <sup>110</sup>C. Hock, J. B. Kim, M. L. Weichman, T. I. Yacovitch, and D. M. Neumark, *J. Chem. Phys.* **137**, 244201 (2012).
- <sup>111</sup>M. L. Weichman and D. M. Neumark, *Annu. Rev. Phys. Chem.* **69**, 101 (2018).
- <sup>112</sup>T. N. Kitsopoulos, I. M. Waller, J. G. Loeser, and D. M. Neumark, *Chem. Phys. Lett.* **159**, 300 (1989).
- <sup>113</sup>E. P. Wigner, *Phys. Rev.* **73**, 1002 (1948).
- <sup>114</sup>M. J. Nee, A. Osterwalder, J. Zhou, and D. M. Neumark, *J. Chem. Phys.* **125**, 014306 (2006).
- <sup>115</sup>D. M. Neumark, *J. Phys. Chem. A* **112**, 13287 (2008).
- <sup>116</sup>J. A. de Vine, M. L. Weichman, B. Laws, J. Chang, M. C. Babin, G. Balerdi, C. Xie, C. L. Malbon, W. C. Lineberger, D. R. Yarkony, R. W. Field, S. T. Gibson, J. Ma, H. Guo, and D. M. Neumark, *Science* **358**, 336 (2017).
- <sup>117</sup>C. J. Hammond and K. L. Reid, *Phys. Chem. Chem. Phys.* **10**, 6762 (2008).
- <sup>118</sup>A. Sanov and W. Carl Lineberger, *Phys. Chem. Chem. Phys.* **6**, 2018 (2004).
- <sup>119</sup>A. E. Bragg, J. R. R. Verlet, A. Kammrath, O. Cheshnovsky, and D. M. Neumark, *J. Chem. Phys.* **122**, 054314 (2005).
- <sup>120</sup>J. R. R. Verlet, A. E. Bragg, A. Kammrath, O. Cheshnovsky, and D. M. Neumark, *J. Chem. Phys.* **121**, 10015 (2004).
- <sup>121</sup>A. Stolow, A. E. Bragg, and D. M. Neumark, *Chem. Rev.* **104**, 1719 (2004).
- <sup>122</sup>R. Spesyvtsev, J. G. Underwood, and H. H. Fielding, "Time-resolved photoelectron spectroscopy for excited state dynamics," in *Ultrafast Phenomena in Molecular Sciences*, Springer Series in Chemical Physics, Vol. 107, edited by R. de Nalda and L. Bañares (Springer, Cham, 2014).
- <sup>123</sup>T. Jian, X. Chen, S.-D. Li, A. I. Boldyrev, J. Li, and L.-S. Wang, *Chem. Soc. Rev.* **48**, 3550 (2019).



- <sup>124</sup>C. D. Sherrill, D. E. Manolopoulos, T. J. Martínez, and A. Michaelides, *J. Chem. Phys.* **153**, 070401 (2020).
- <sup>125</sup>R. N. Schaugaard, J. E. Topolski, M. Ray, K. Raghavachari, and C. C. Jarrold, *J. Chem. Phys.* **148**, 054308 (2018).
- <sup>126</sup>S. Gozem, P. Wojcik, V. Mozhaynskiy, and A. Krylov, <http://iopshell.usc.edu/downloads>.
- <sup>127</sup>J. V. Ortiz, *J. Chem. Phys.* **153**, 070902 (2020).
- <sup>128</sup>T.-C. Jagau and A. I. Krylov, *J. Chem. Phys.* **144**, 054113 (2016).
- <sup>129</sup>L. M. Thompson, H. Harb, and H. P. Hratchian, *J. Chem. Phys.* **144**, 204117 (2016).
- <sup>130</sup>H. Harb and H. P. Hratchian, *J. Chem. Phys.* **154**, 084104 (2021).
- <sup>131</sup>J. L. Mason, H. Harb, C. D. Huizenga, J. C. Ewigleben, J. E. Topolski, H. P. Hratchian, and C. C. Jarrold, *J. Phys. Chem. A* **123**, 2040 (2019).
- <sup>132</sup>L. M. Thompson, C. C. Jarrold, and H. P. Hratchian, *J. Chem. Phys.* **146**, 104301 (2017).
- <sup>133</sup>K. M. McHugh, J. G. Eaton, G. H. Lee, H. W. Sarkas, L. H. Kidder, J. T. Snodgrass, M. R. Manaa, and K. H. Bowen, *J. Chem. Phys.* **91**, 3792 (1989).
- <sup>134</sup>H. Choi, R. T. Bise, A. A. Hoops, and D. M. Neumark, *J. Chem. Phys.* **113**, 2255 (2000).
- <sup>135</sup>A. S. Ivanov, X. Zhang, H. Wang, A. I. Boldyrev, G. Ganteför, K. H. Bowen, and I. Černušák, *J. Phys. Chem. A* **119**, 11293 (2015).
- <sup>136</sup>W. Weltner, Jr. and R. J. Van Zee, *Chem. Rev.* **89**, 1713 (1989).
- <sup>137</sup>G. Meloni, M. J. Ferguson, S. M. Sheehan, and D. M. Neumark, *Chem. Phys. Lett.* **399**, 389 (2004).
- <sup>138</sup>C. C. Arnold and D. M. Neumark, *J. Chem. Phys.* **99**, 3353 (1993).
- <sup>139</sup>X. Wu, X. Liang, Q. Du, J. Zhao, M. Chen, M. Lin, J. Wang, G. Yin, L. Ma, R. B. King, and B. von Issendorff, *J. Phys.: Condens. Matter* **30**, 354002 (2018).
- <sup>140</sup>G. R. Burton, C. Xu, and D. M. Neumark, *Surf. Rev. Lett.* **03**, 383 (1996).
- <sup>141</sup>G. R. Burton, C. Xu, C. C. Arnold, and D. M. Neumark, *J. Chem. Phys.* **104**, 2757 (1996).
- <sup>142</sup>L.-F. Cui, L.-M. Wang, and L.-S. Wang, *J. Chem. Phys.* **126**, 064505 (2007).
- <sup>143</sup>V. D. Moravec, S. A. Klopčič, and C. C. Jarrold, *J. Chem. Phys.* **110**, 5079 (1999).
- <sup>144</sup>L.-F. Cui, X. Huang, L.-M. Wang, J. Li, and L.-S. Wang, *J. Phys. Chem. A* **110**, 10169 (2006).
- <sup>145</sup>Y. Negishi, H. Kawamata, A. Nakajima, and K. Kaya, *J. Electron Spectrosc. Relat. Phenom.* **106**, 117 (2000).
- <sup>146</sup>D. W. Arnold, S. E. Bradforth, T. N. Kitsopoulos, and D. M. Neumark, *J. Chem. Phys.* **95**, 8753 (1991).
- <sup>147</sup>V. Senz, T. Fischer, P. Oelßner, J. Tiggesbäumker, J. Stanzel, C. Bostedt, H. Thomas, M. Schöffler, L. Foucar, M. Martins, J. Nevile, M. Neeb, T. Möller, W. Wurth, E. Rühl, R. Dörner, H. Schmidt-Böcking, W. Eberhardt, G. Ganteför, R. Treusch, P. Radcliffe, and K.-H. Meiwes-Broer, *Phys. Rev. Lett.* **102**, 138303 (2009).
- <sup>148</sup>D. C. Conway, *J. Chem. Phys.* **50**, 3864 (1969).
- <sup>149</sup>C. R. Sherwood, M. C. Garner, K. A. Hanold, K. M. Strong, and R. E. Continetti, *J. Chem. Phys.* **102**, 6949 (1995).
- <sup>150</sup>K. M. Patros, J. E. Mann, and C. C. Jarrold, *J. Phys. Chem. A* **120**, 7828 (2016).
- <sup>151</sup>T. P. Lippa, S.-J. Xu, S. A. Lyapustina, J. M. Nilles, and K. H. Bowen, *J. Chem. Phys.* **109**, 10727 (1998).
- <sup>152</sup>R. O. Jones, G. Ganteför, s. Hunsicker, and P. Pieperhoff, *J. Chem. Phys.* **103**, 9549 (1995).
- <sup>153</sup>J. B. Kim, C. Hock, T. I. Yacovitch, and D. M. Neumark, *J. Phys. Chem. A* **117**, 8126 (2013).
- <sup>154</sup>L. S. Wang, *Int. Rev. Phys. Chem.* **35**, 69 (2016).
- <sup>155</sup>A. P. Sergeeva, Z. A. Piazza, C. Romanescu, W.-L. Li, A. I. Boldyrev, and L.-S. Wang, *J. Am. Chem. Soc.* **134**, 18065 (2012).
- <sup>156</sup>T.-T. Chen, W.-L. Li, T. Jian, X. Chen, J. Li, and L.-S. Wang, *Angew. Chem., Int. Ed.* **129**, 7020 (2017).
- <sup>157</sup>H.-J. Zhai, Y.-F. Zhao, W.-L. Li, Q. Chen, H. Bai, H.-S. Hu, Z. A. Piazza, W.-J. Tian, H.-G. Lu, Y.-B. Wu, Y.-W. Mu, G.-F. Wei, Z.-P. Liu, J. Li, S.-D. Li, and L.-S. Wang, *Nat. Chem.* **6**, 727 (2014).
- <sup>158</sup>G. Ganteför, M. Gausa, K. H. Meiwes-Broer, and H. O. Lutz, *Z. Phys. D: At., Mol. Clusters* **9**, 253 (1988).
- <sup>159</sup>J. Akola, M. Manninen, H. Häkkinen, U. Landman, X. Li, and L.-S. Wang, *Phys. Rev. B* **60**, R11297 (1999).
- <sup>160</sup>J. Akola, M. Manninen, H. Häkkinen, U. Landman, X. Li, and L.-S. Wang, *Phys. Rev. B* **62**, 13216 (2000).
- <sup>161</sup>C.-Y. Cha, G. Ganteför, and W. Eberhardt, *Ber. Bunsenges. Phys. Chem.* **96**, 1223 (1992).
- <sup>162</sup>W. D. Knight, W. A. de Heer, W. A. Saunders, K. Clemenger, M. Y. Chou, and M. L. Cohen, *Chem. Phys. Lett.* **134**, 1 (1987).
- <sup>163</sup>P. Milani, W. de Heer, and A. Châtelain, *Z. Phys. D: At., Mol. Clusters* **19**, 133 (1991).
- <sup>164</sup>L. Ma, B. v. Issendorff, and A. Aguado, *J. Chem. Phys.* **132**, 104303 (2010).
- <sup>165</sup>S.-J. Xu, J. M. Nilles, D. Radisic, W.-J. Zheng, S. Stokes, K. H. Bowen, R. C. Becker, and I. Boustani, *Chem. Phys. Lett.* **379**, 282 (2003).
- <sup>166</sup>O. C. Thomas, W.-J. Zheng, T. P. Lippa, S.-J. Xu, S. A. Lyapustina, and K. H. Bowen, *J. Chem. Phys.* **114**, 9895 (2001).
- <sup>167</sup>A. W. Castleman and S. N. Khanna, *J. Phys. Chem. C* **113**, 2664 (2009).
- <sup>168</sup>P. Jena and Q. Sun, *Chem. Rev.* **118**, 5755 (2018).
- <sup>169</sup>C. Liu, B. Yang, E. Tyo, S. Seifert, J. Debartolo, B. Von Issendorff, P. Zapol, S. Vajda, and L. A. Curtiss, *J. Am. Chem. Soc.* **137**, 8676 (2015).
- <sup>170</sup>H. Fang and P. Jena, *J. Mater. Chem. A* **4**, 4728 (2016).
- <sup>171</sup>S. Giri, S. Behera, and P. Jena, *Angew. Chem., Int. Ed.* **53**, 13916 (2014).
- <sup>172</sup>K. M. Ervin, J. Ho, and W. C. Lineberger, *J. Chem. Phys.* **89**, 4514 (1988).
- <sup>173</sup>O. Cheshnovsky, K. J. Taylor, J. Conceicao, and R. E. Smalley, *Phys. Rev. Lett.* **64**, 1785 (1990).
- <sup>174</sup>L.-S. Wang and H. Wu, *Z. Phys. Chem.* **203**, 45 (1998).
- <sup>175</sup>K. J. Taylor, C. L. Pettiette-Hall, O. Cheshnovsky, and R. E. Smalley, *J. Chem. Phys.* **96**, 3319 (1992).
- <sup>176</sup>O. C. Thomas, W. Zheng, S. Xu, and K. H. Bowen, *Phys. Rev. Lett.* **89**, 213403 (2002).
- <sup>177</sup>S.-R. Liu, H.-J. Zhai, and L.-S. Wang, *J. Chem. Phys.* **117**, 9758 (2002).
- <sup>178</sup>M. Haruta, *Catal. Today* **36**, 153 (1997).
- <sup>179</sup>J. Li, X. Li, H. J. Zhai, and L. S. Wang, *Science* **299**, 864 (2003).
- <sup>180</sup>W. Huang and L.-S. Wang, *Phys. Rev. Lett.* **102**, 153401 (2009).
- <sup>181</sup>N. Shao, W. Huang, Y. Gao, L.-M. Wang, X. Li, L.-S. Wang, and X. C. Zeng, *J. Am. Chem. Soc.* **132**, 6596–6605 (2010).
- <sup>182</sup>B. Schaefer, R. Pal, N. S. Khetrapal, M. Amsler, A. Sadeghi, V. Blum, X. C. Zeng, S. Goedecker, and L.-S. Wang, *ACS Nano* **8**, 7413 (2014).
- <sup>183</sup>W. Huang, S. Bulusu, R. Pal, X. C. Zeng, and L.-S. Wang, *ACS Nano* **3**, 1225 (2009).
- <sup>184</sup>H. Häkkinen, M. Moseler, and U. Landman, *Phys. Rev. Lett.* **89**, 033401 (2002).
- <sup>185</sup>A. Lechtken, C. Neiss, M. M. Kappes, and D. Schooss, *Phys. Chem. Chem. Phys.* **11**, 4344 (2009).
- <sup>186</sup>R. Kelting, A. Baldes, U. Schwarz, T. Rapps, D. Schooss, P. Weis, C. Neiss, F. Weigend, and M. M. Kappes, *J. Chem. Phys.* **136**, 154309 (2012).
- <sup>187</sup>E. Waldt, A.-S. Hehn, R. Ahlrichs, M. M. Kappes, and D. Schooss, *J. Chem. Phys.* **142**, 024319 (2015).
- <sup>188</sup>H. Weidele, D. Kreisle, E. Recknagel, G. Schulze Icking-Konert, H. Handschuh, G. Ganteför, and W. Eberhardt, *Chem. Phys. Lett.* **237**, 425 (1995).
- <sup>189</sup>G. Ganteför, W. Eberhardt, H. Weidele, D. Kreisle, and E. Recknagel, *Phys. Rev. Lett.* **77**, 4524 (1996).
- <sup>190</sup>B. Bagueard, J. C. Pinaré, C. Bordas, and M. Broyer, *Phys. Rev. A* **63**, 023204 (2001).
- <sup>191</sup>J. Heinzelmänn, P. Kruppa, S. Proch, Y. D. Kim, and G. Ganteför, *Chem. Phys. Lett.* **603**, 1 (2014).
- <sup>192</sup>R. M. Young, G. B. Griffin, O. T. Ehrler, A. Kammrath, A. E. Bragg, J. R. R. Verlet, O. Cheshnovsky, and D. M. Neumark, *Phys. Scr.* **80**, 048102 (2009).
- <sup>193</sup>A. Koop, G. Ganteför, and Y. D. Kim, *Phys. Chem. Chem. Phys.* **19**, 21335 (2017).
- <sup>194</sup>A. Kunin and D. M. Neumark, “Femtosecond time-resolved photoelectron spectroscopy of molecular anions,” in *Physical Chemistry of Cold Gas-Phase Functional Molecules and Clusters*, edited by T. Ebata and M. Fujii (Springer, Singapore, 2019).
- <sup>195</sup>D. W. Rothgeb, E. Hossain, A. T. Kuo, J. L. Troyer, and C. C. Jarrold, *J. Chem. Phys.* **131**, 044310 (2009).

- <sup>196</sup>D. W. Rothgeb, J. E. Mann, S. E. Waller, and C. C. Jarrold, *J. Chem. Phys.* **135**, 104312 (2011).
- <sup>197</sup>J. E. Mann, S. E. Waller, D. W. Rothgeb, and C. Chick Jarrold, *J. Chem. Phys.* **135**, 104317 (2011).
- <sup>198</sup>B. L. Yoder, J. T. Maze, K. Raghavachari, and C. C. Jarrold, *J. Chem. Phys.* **122**, 094313 (2005).
- <sup>199</sup>J. E. Mann, D. W. Rothgeb, S. E. Waller, and C. C. Jarrold, *J. Phys. Chem. A* **114**, 11312 (2010).
- <sup>200</sup>S. E. Waller, J. E. Mann, E. Hossain, M. Troyer, and C. C. Jarrold, *J. Chem. Phys.* **137**, 024302 (2012).
- <sup>201</sup>S. E. Waller, J. E. Mann, D. W. Rothgeb, and C. C. Jarrold, *J. Phys. Chem. A* **116**, 9639 (2012).
- <sup>202</sup>J. E. Mann, S. E. Waller, and C. C. Jarrold, *J. Phys. Chem. A* **117**, 12116 (2013).
- <sup>203</sup>N. J. Mayhall, D. W. Rothgeb, E. Hossain, K. Raghavachari, and C. C. Jarrold, *J. Chem. Phys.* **130**, 124313 (2009).
- <sup>204</sup>H. W. Sarkas, L. H. Kidder, and K. H. Bowen, *J. Chem. Phys.* **102**, 57 (1995).
- <sup>205</sup>A. N. Alexandrova, A. I. Boldyrev, Y.-J. Fu, X. Yang, X.-B. Wang, and L.-S. Wang, *J. Chem. Phys.* **121**, 5709 (2004).
- <sup>206</sup>N. O. Jones, S. N. Khanna, T. Baruah, M. R. Pederson, W. J. Zheng, J. M. Nilles, and K. H. Bowen, *Phys. Rev. B* **70**, 134422 (2004).
- <sup>207</sup>J. E. Mann, N. J. Mayhall, and C. C. Jarrold, *Chem. Phys. Lett.* **525-526**, 1 (2012).
- <sup>208</sup>M. Ray, J. A. Felton, J. O. Kafader, J. E. Topolski, and C. C. Jarrold, *J. Chem. Phys.* **142**, 064305 (2015).
- <sup>209</sup>J. E. Topolski, J. O. Kafader, V. Marrero-Colon, S. S. Iyengar, H. P. Hratchian, and C. C. Jarrold, *J. Chem. Phys.* **149**, 054305 (2018).
- <sup>210</sup>J. O. Kafader, M. Ray, and C. C. Jarrold, *J. Chem. Phys.* **143**, 034305 (2015).
- <sup>211</sup>J. O. Kafader, M. Ray, and C. C. Jarrold, *J. Chem. Phys.* **143**, 064305 (2015).
- <sup>212</sup>M. Ray, J. O. Kafader, J. E. Topolski, and C. C. Jarrold, *J. Chem. Phys.* **145**, 044317 (2016).
- <sup>213</sup>J. O. Kafader, J. E. Topolski, and C. C. Jarrold, *J. Chem. Phys.* **145**, 154306 (2016).
- <sup>214</sup>J. O. Kafader, J. E. Topolski, V. Marrero-Colon, S. S. Iyengar, and C. C. Jarrold, *J. Chem. Phys.* **146**, 194310 (2017).
- <sup>215</sup>J. L. Mason, J. E. Topolski, J. Ewigleben, S. S. Iyengar, and C. C. Jarrold, *J. Phys. Chem. Lett.* **10**, 144 (2019).
- <sup>216</sup>N. N. Negulyaev, V. S. Stepanyuk, W. Hergert, and J. Krischner, *Phys. Rev. Lett.* **106**, 0037202 (2011).
- <sup>217</sup>P. Koirala, B. Kiran, A. K. Kandalam, C. A. Fancher, H. L. de Clercq, X. Li, and K. H. Bowen, *J. Chem. Phys.* **135**, 134311 (2011).
- <sup>218</sup>S. Gemming, J. Tamuliene, G. Seifert, N. Bertram, Y. D. Kim, and G. Ganteför, *Appl. Phys. A* **82**, 161 (2006).
- <sup>219</sup>D. E. Clemmer, J. M. Hunter, K. B. Shelimov, and M. F. Jarrold, *Nature* **372**, 248 (1994).
- <sup>220</sup>B. D. Leskiw and A. W. Castleman, *C. R. Phys.* **3**, 251 (2002).
- <sup>221</sup>S. Li, H. Wu, and L.-S. Wang, *J. Am. Chem. Soc.* **119**, 7417 (1997).
- <sup>222</sup>Y. Chai, T. Guo, C. Jin, R. E. Haufler, L. P. F. Chibante, J. Fure, L. Wang, J. M. Alford, and R. E. Smalley, *J. Phys. Chem.* **95**, 7564 (1991).
- <sup>223</sup>J. Zhao, Q. Du, S. Zhou, and V. Kumar, *Chem. Rev.* **120**, 9021 (2020).
- <sup>224</sup>X.-L. Xu, B. Yang, C.-J. Zhang, H.-G. Xu, and W.-J. Zheng, *J. Chem. Phys.* **150**, 074304 (2019).
- <sup>225</sup>H.-G. Xu, Z.-G. Zhang, Y. Feng, J. Yuan, Y. Zhao, and W. Zheng, *Chem. Phys. Lett.* **487**, 204 (2010).
- <sup>226</sup>B. Yang, X.-L. Xu, H.-G. Xu, U. Farooq, and W.-J. Zheng, *Phys. Chem. Chem. Phys.* **21**, 6207 (2019).
- <sup>227</sup>X.-J. Deng, X.-Y. Kong, H.-G. Xu, X.-L. Xu, G. Feng, and W.-J. Zheng, *J. Phys. Chem. C* **119**, 11048 (2015).
- <sup>228</sup>X. Xia, Z.-G. Zhang, H.-G. Xu, X. Xu, X. Kuang, C. Lu, and W. Zheng, *Phys. Chem. C* **123**, 1931 (2019).
- <sup>229</sup>X. Zhang, Y. Wang, H. Wang, A. Lim, G. Gantefoer, K. H. Bowen, J. U. Reveles, and S. N. Khanna, *J. Am. Chem. Soc.* **135**, 4856 (2013).
- <sup>230</sup>I. A. Popov, T. Jian, G. V. Lopez, A. I. Boldyrev, and L. S. Wang, *Nat. Commun.* **6**, 8654 (2015).
- <sup>231</sup>L. F. Cheung, T.-T. Chen, G. S. Kocheril, W.-J. Chen, J. Czekner, and L.-S. Wang, *J. Phys. Chem. Lett.* **11**, 659 (2020).
- <sup>232</sup>X. Chen, T.-T. Chen, W.-L. Li, J.-B. Lu, L.-J. Zhao, T. Jian, H.-S. Hu, L.-S. Wang, and J. Li, *Inorg. Chem.* **58**, 411 (2019).
- <sup>233</sup>L. F. Cheung, G. S. Kocheril, J. Czekner, and L.-S. Wang, *J. Phys. Chem. A* **124**, 2820 (2020).
- <sup>234</sup>P. J. Robinson, X. Zhang, T. McQueen, K. H. Bowen, and A. N. Alexandrova, *J. Phys. Chem. A* **121**, 1849 (2017).
- <sup>235</sup>T.-T. Chen, W.-L. Li, W.-J. Chen, J. Li, and L.-S. Wang, *Chem. Commun.* **55**, 7864 (2019).
- <sup>236</sup>X. Zhang, P. J. Robinson, G. Gantefoer, A. Alexandrova, and K. H. Bowen, *J. Chem. Phys.* **143**, 094307 (2015).
- <sup>237</sup>Z. Liu, Y. Bai, Y. Li, J. He, Q. Lin, H. Xie, and Z. Tang, *Phys. Chem. Chem. Phys.* **22**, 23773 (2020).
- <sup>238</sup>J. Stanzel, E. F. Aziz, M. Neeb, and W. Eberhardt, *Chem. Commun.* **72**, 1 (2007).
- <sup>239</sup>B. Chatterjee, F. A. Akin, C. C. Jarrold, and K. Raghavachari, *J. Chem. Phys.* **119**, 10591 (2003).
- <sup>240</sup>S. A. Klopčič, V. D. Moravec, and C. C. Jarrold, *J. Chem. Phys.* **110**, 8986 (1999).
- <sup>241</sup>V. D. Moravec and C. C. Jarrold, *J. Chem. Phys.* **112**, 792 (2000).
- <sup>242</sup>G. Liu, S. M. Ciburowski, Z. Zhu, and K. H. Bowen, *Int. J. Mass Spec.* **435**, 114 (2019).
- <sup>243</sup>M. Gerhards, O. C. Thomas, J. M. Nilles, W.-J. Zheng, and K. H. Bowen, *J. Chem. Phys.* **116**, 10247 (2002).
- <sup>244</sup>E. Hossain and C. C. Jarrold, *J. Chem. Phys.* **130**, 064301 (2009).
- <sup>245</sup>Z. Liu, Y. Bai, Y. Li, J. He, Q. Lin, L. Hou, H.-S. Wu, F. Zhang, J. Jia, H. Xie, and Z. Tang, *Dalton Trans.* **49**, 15256 (2020).
- <sup>246</sup>H. Xie, J. Zou, Q. Yuan, H. Fan, Z. Tang, and L. Jiang, *J. Chem. Phys.* **144**, 124303 (2016).
- <sup>247</sup>Q. Yuan, W. Cao, and X.-B. Wang, *Int. Rev. Phys. Chem.* **39**, 83 (2020).
- <sup>248</sup>G. Liu, V. Chauhan, A. P. Aydt, S. M. Ciburowski, A. Pinkard, Z. Zhu, X. Roy, S. N. Khanna, and K. H. Bowen, *J. Phys. Chem. C* **123**, 25121 (2019).
- <sup>249</sup>G. Liu, A. Pinkard, S. M. Ciburowski, V. Chauhan, Z. Zhu, A. P. Aydt, S. N. Khanna, X. Roy, and K. H. Bowen, *Chem. Sci.* **10**, 1760 (2019).
- <sup>250</sup>K. Hirata, K. Kim, K. Nakamura, H. Kitazawa, S. Hayashi, K. Koyasu, and T. Tsukuda, *J. Phys. Chem. C* **123**, 13174 (2019).
- <sup>251</sup>L. Ma, R. Moro, J. Bowlan, A. Kirilyuk, and W. A. de Heer, *Phys. Rev. Lett.* **113**, 157203 (2014).
- <sup>252</sup>J. Bahn, P. Oelßner, M. Köther, C. Braun, V. Senz, S. Palutke, M. Martins, E. Rühl, G. Ganteför, T. Möller, B. von Issendorff, D. Bauer, J. Tiggesbäumker, and K.-H. Meiwes-Broer, *New J. Phys.* **14**, 075008 (2012).
- <sup>253</sup>L. Wu, C. Zhang, S. A. Krasnokutski, and D.-S. Yang, *J. Chem. Phys.* **140**, 224307 (2014).
- <sup>254</sup>W. E. Kaden, W. A. Kunkel, F. S. Roberts, M. Kane, and S. L. Anderson, *J. Chem. Phys.* **136**, 204705 (2012).
- <sup>255</sup>W. E. Kaden, W. A. Kunkel, F. S. Roberts, M. Kane, and S. L. Anderson, *Surf. Sci.* **621**, 40 (2014).
- <sup>256</sup>L. Howard-Fabretto and G. G. Andersson, *Adv. Mater.* **32**, 1904122 (2020).
- <sup>257</sup>R. E. Palmer, R. Cai, and J. Vernieres, *Acc. Chem. Res.* **51**, 2296 (2018).
- <sup>258</sup>X. Tang, X. Li, K. Wepasnick, A. Lim, D. H. Fairbrother, K. H. Bowen, T. Mangler, S. Noessner, C. Wolke, M. Grossmann, A. Koop, G. Gantefoer, B. Kiran, and A. K. Kandalam, *J. Phys.: Conf. Ser.* **438**, 012005 (2013).
- <sup>259</sup>W. E. Ernst and A. W. Hauser, *Phys. Chem. Chem. Phys.* **23**, 7553 (2021).
- <sup>260</sup>L. Kazak, S. Göde, K.-H. Meiwes-Broer, and J. Tiggesbäumker, *J. Phys. Chem. A* **123**, 5951 (2019).